Authors response to the comments of referee #1

We thank referee #1 for the thorough and insightful review of the manuscript. The reviewer criticized our description of the methodology, the missing information concerning our error estimates, the validation by kinematic GNSS profiles only and the lack of 'numbers to back up most of the statements made'.

We have put much effort in rewriting the respective sections and think that this contributed to a much clearer presentation of the methodology and the results now. In order to describe the methodology in more detail, we have added significantly more details in the supplementary. We think that this is a good compromise between keeping the manuscript itself relatively short for the majority of the readers but having all technical details available for everybody who is interested. Error estimates have always been part of our processing but we agree, they have to be given their space in the manuscript as well. Therefore, we added respectively short descriptions in the manuscript as well as further details in the supplement.

Also the validation with IceBridge has been included now. However, we would like to stress that we are comparing the absolute elevation differences between two epochs. The magnitude of the difference is not important for this validation. Nevertheless, we agree that IceBridge contributes significantly more validation data in areas with complex topographies. Hence, this validation indeed provided important information. We included this validation but added a slope dependency to account for the topography effects.

To provide more 'quantitative facts' we added several correlation coefficients and key numbers. However, one of the major benefits of this work is the high temporal sampling of processes. Single numbers as linear trends, or even acceleration rates, can not always describe the underlying processes adequately.

Besides addressing these key issues, a major change in the revised version is that we have converted the volume changes into mass changes. With respect to some of the specific comments below, this indeed makes the comparison with the external data sets more meaningful, compared to the earlier version of the manuscript. We have decided for a rather straightforward and robust density mask approach, allowing us to still compare the SMBs as independent data set.

In the following we will respond the specific comments one by one.

Comment 1: Abstract – The abstract is quite long, but not well written. About half of the text is spent discussing the percent coverage for the 25 year and 40 year epochs, however these numbers aren't key scientific results so would be better placed in the data or methods section. Additionally, the coverage stats are poorly defined here, for example is this the percent coverage that of the raw data, plane fit output at whatever grid resolution used, or the extrapolated interpolated result. Without being specific the coverage stats are open to misinterpretation.
The abstract has been completely redesigned, being more focused. Besides the abstract, more details on our definition of 'observed' cells have been added in Sect. 3.3.3 and 5.2.

Comment 2: Abstract - The title of the paper states that this paper is about surface elevation change, but there are no key surface elevation change numbers stated in the abstract. Why not, if this is the main purpose of the paper?
The main focus of this paper are the time series of surface elevation change from multi-mission altimetry. We show that surface elevation changes are much more complex than just a single rate or even an acceleration. These variation are shown on a spatial and a temporal scale in the results section. In our revised version, we added a key value for the total mass change of the AIS since 1992 but also discuss the importance of the time series.

Comment 3: Abstract – The second paragraph of the abstract lacks any quantitative facts. For example, Pg1 L14 states that surface elevation change shows 'high coincidence' with precipitation anomalies and gravimetry; Pg1 L16 states that there is a 'high level' of agreement; and Pg1 L18 states that 'Geosat coincides very well with. . .'. The authors should replace these generic adjectives with quantitative statistics to back up their statements.
Respective correlation coefficients have been included in the document, but the respective sentence is no longer part of the abstract.

Comment 4: Abstract – Pg1 L15 – 'Satellite gravimetry' is the technique, but the authors have presumably compared their elevation results against a derived product, such as mass loss. Edit wording to be precise.
We agree, but in the revised version, this is no longer part of the abstract.

Comment 5: Abstract – Pg1 L18 – The Seasat and Geosat altimeters operated at radar frequencies and will consequently penetrate some depth into the snowpack, its therefore not a given that the elevation trend from these satellites should correlate with precipitation anomalies in snowfall. The penetration depth is spatially and temporally variable, influenced by snow density and moisture content. As the radar return originates from a scattering horizon within the snowpack, correlation between precipitation anomalies and rates of elevation change can't prove that the elevation change trends are 'reliable', so the satellite based elevation trends must be verified with a comparable elevation change dataset.
The penetration depth variations have been accounted for by the backscatter correction in Eq. (2) (except for Seasat, where the time period is too short). The offset corrections align the scattering horizons of the different missions. Section D in our revised supplement shows that the trend-corrected anomalies of the FDM and of the SEC differ by 0.12 ± 0.21 cm for Geosat and 0.26 ± 0.32 cm for Seasat (including one year without observations). Considering that the model is prone to some uncertainties as well, we think that this agreement is remarkable.

Comment 6: P1 L21 – Sentence wording not correct English, edit required. The wording throughout this paragraph is poor.
The introduction has been completely rewritten.

Comment 7: P1 L22 – Does the author mean sequentially rather than concurrently?
The introduction has been completely rewritten.

Comment 8: P2 L6 – Edit wording to say precisely what is meant. A long time series would not have prevented Wingham observing negative elevation rates in Dronning Maud Land compared with Flaments positive result for the same area, because as stated the observational time period is different. 'Help reduce the influence of such events' is factually incorrect.
The introduction has been completely rewritten.

Comment 9: P2 L10 – Edit wording. Mission calibration doesn't become 'more important', it is maybe more challenging though.
Changed.

Comment 10: P2, Fig1 – Add separate colorbar for map of spatial coverage as currently hard to interpret. Just the circle out- line that corresponds to bar color, but really hard to see in pole hole.
Changed.

Comment 11: P3 L1 – Edit wording to be more precise. As the raw data from both satellites was acquired in the same pulse limited imaging mode, the use of the word 'mode' to describe a processing choice could be misinterpreted. Additionally I think the two modes authors are talking about are ocean and ice retrackers, however there are actually 3 retrackers available for these missions (ice-1 and ice-2 are separate).
There seems to be a misunderstanding. The measurements of ERS have been switched between 'ice' and 'ocean' mode. See Paolo et al. (2016): 'To improve performance over the ice sheets, ERS-1 and ERS-2 operated in both a standard 'ocean mode' and a specialized 'ice mode', with mode switching based on an ocean-ice mask. For ice mode, the 64-bin range window (the segment of return echo that is recorded) was four times wider than for ocean mode (116.48 m vs 29.12 m), increasing the chances of capturing return signals over rough topographic surfaces.' We changed the wording to give a more self-contained explanation.

Comment 12: P3 L3 – Paolo et al presents results over flat ice shelves with zero slope, whereas this paper presents results over an ice sheet, where the most rapidly changing regions are found in the most steeply sloping terrain. The logic that Paolo used to justify including data from different imaging modes therefore may not apply to this paper. The authors should use data from a single retracker which has been shown to be more reliable, or quantitatively justify why including less reliable data improves the quality of the end elevation change result. E.g. via coverage, temporal extent, or reduced error maybe. It follows that a separate error estimate should be provided for the

elevation change result derived from different quality input datasets.
In this comment 'observation mode' and 'retracker' seems to be mixed up again. The retracker is a post-processing step, applied to the observed waveform. In contrast, one of the main differences between the observation modes is the onboard sampling of this waveform (see answer to comment 11). This question obviously refers to the observation modes. Both modes have been treated as independent data sets. For ERS-1 and ERS-2, we used individual a priori uncertainty estimates in the repeat altimetry processing (Eq. 2), estimated individual mission parameters and applied individual offsets. For each epoch where both modes exist, the monthly mean values have their individual error estimate. Hence, in the PLRA averaging step (Sect. 3.3.1), which combines the data, a poor quality of any mode would be reflected by a high RMS and, hence, a low weight in the average. We see no reason why we should remove one observation mode completely. A further discussion to the respective modes has been added in C.2.

Comment 13: P3 L4 – Specify the size of the bias between both modes, for both satellites.
This is done later in Sect. 3.3.1. The bias can be seen at Fig. S3.

Comment 14: P3 L16 – The Helm et al DEM is the ice surface during the first 3 years of CryoSat, however this surface has changed significantly in many regions throughout the 40-year study period. The ice surface of the DEM should evolve temporally to reflect the known elevation change, otherwise the slope correction will not be correct. This effect will be significant in regions such as WAIS which have shown to thin at a maximum rates of up to 9 m/yr. Have the authors done this, or if not what is the error on the slope correction that will result from not temporally evolving the ice surface for 40 years?
The absolute elevation of the topography has only a negligible influence on the location of the POCA. The POCA mainly depends on the relative topography, that is, the variations of topography w.r.t. the mean, over the footprint. If any changes of this relative topography occur, their rates are significantly lower than the rates of the mean absolute topography change (at least in regions that can be observed by pulse limited radar altimetry at all). Hence, we agree that such an effect exists, but its influence on the location of the POCA is negligible.

Comment 15: P3 L29 – Can the authors quantitatively state how much less sensitive to noise the OCOG retracker is compared to other options, and does this affect all satellites the same way given that the spatial resolution and imaging modes are different. Some retrackers will perform better over different terrain types (sloping or flat), therefore it would be helpful for more details to be provided about the region, time period, and satellites for which this analysis was performed.
Details on the comparison between functional fit and threshold retrackers have been added to Tab.1. The noise of different retrackers has been discussed in Schröder et al. (2017) as well, to which we refer at the respective locations here. Concerning the comparison between a waveform maximum and a OCOG threshold retracker, Bamber (1994) explain that the single 'maximum bin' is significantly more affected by noise as the squared mean over all bins. However, we did not apply this option, so we cannot provide any numbers.

Comment 16: P4 L3 – If the CryoSat retracking doesn't exactly replicate the methods in Helm et al, the full details should be detailed in this paper.
The retracking of the CryoSat-2 SARIn data was the method of Helm et al. (2014). We changed the wording to make this more clear.

Comment 17: P4 L13 – It is well known (as the authors later state) that anisotropy exists between ascending and descending tracks of radar altimetry data, and indeed many elevation change papers include a term for this in the plane fit solution to exclude any bias from this. When calculating data precision from ascending and descending tracks have the authors performed such a correction, and if so could further detail be provided on its size per mission.
We did not apply such a correction, but showed how the A-D bias is reduced by our low threshold retracker. Consequently, the precision from ascending-descending crossover differences includes the effect of the A-D bias as well. Table 1 and Fig. S2 show how the precision (including the effect of the A-D bias) is improved for each mission.

Comment 18: P5 L5 – Edit text to state quantitative statistics about the absolute or percent improvement following their slope correction. Frustrating that 'superior performance' and 'similar improvements' used when a number would be more persuasive.

Numbers added and text modified.

Comment 19: P5 L17 – Figure S1 does show a reduction in the anisotropy effect, but the signal is clearly still present in the data. Additionally, smoothing a result with an artefact in doesn't remove the affected data, so this error will clearly have an effect on the end result. If as the authors state recent previously published studies have designed and successfully implemented an anisotropy correction, this paper should add this step to avoid unnecessary error. If the authors chose not to do this, I would ask that the quantify what the affect of not applying the correction is to prove its not discernable.
Firstly, the mentioned studies use data which have been retracked using a functional fit retracker, where the effect of the A-D bias if much larger (see Fig. S2). Secondly, we do not simply smooth data with a systematic offset. When averaging ascending with descending data (which are both affected by the A-D bias, but with opposite signs), the result will not contain a bias any more. The bias will only affect the resulting uncertainty estimate (see answer to comment 17). We average ascending and descending tracks (with typical cross-track distances of less than 20 km) over 60 km. Hence, we usually average 3x3 ascending and 3x3 descending tracks (over 3 months). This perfect constellation will not always be true but, however, also the alternative, the application of a A-D bias correction might contain some issues. As this discussion belongs to the repeat track processing, we have moved it to C.1 and discussed this point there.

Comment 20: P6 L25 – If there are differences in the processing methods used for different missions as stated, this should be fully specified in the supplementary material. Use of full parameter names as found in the mission meta data will ensure that the methods and results presented are repeatable.
These 'parameters' refer to the parameter fit (Eq. 1). We have rewritten the whole paragraph.

Comment :21 P8 L1 – Spelling
Obsolete due to edits.

Comment 22: P8 L1 – Specify the thresholds and variables against which data is filtered out during the elevation change iterative processing. Are the same values used for all missions?
More details added, moved to suppl. C.1.

Comment 23: P8 L7 – Provide some detail on how the backscatter penetration correction is calculated and applied. E.g. over what epoch?
The backscatter penetration correction is applied according to Eq. (2). For each repeat cell and each mission (except Seasat and ICESat) a parameter dBS was estimated. By not including dBS in Eq. (3), the resulting time series are backscatter corrected. This has been explained in more detail in Sect. 3.2 and a further discussion was added to C.1.

Comment 24: P8 L18 – State threshold used to determine outliers.
Each processing step is described in much more detail now in the supplement.

Comment 25: P9 Fig4 – Red colors in this plot do not print well so can't easily differentiate missions. Change color scale used.
Done.

Comment 26: P9 L3 – The authors are simultaneously arguing that for all of the more recent missions a spatially variable offset correction must be applied as the offset is spatially variable, while stating that for Seaseat and Geosat the offset correction must be a constant because some of the difference could may be real elevation change. If the later is true, why does this not also hold for the more recent missions? The fact that a spatially variable correction can't be or hasn't been calculated doesn't remove the justification for why its needed.
For the recent missions we use overlapping epochs. The differences, used to calibrate these missions, refer to the same time (within one month), hence, real elevation changes do not play a significant role here. We believe that the true offsets between Seasat/Geosat and Envisat are spatially variable, just as the offsets between ERS-1/ERS-2/CryoSat-2 LRM and Envisat. However, in contrast to ERS-1/ERS-2/CryoSat-2 LRM, we are not able to estimate the spatially variable offsets for Seasat and Geosat over their region of coverage. This is because Seasat and Geosat have no temporal overlap to the later missions, so that actual elevation changes between the mission times are an additional source of error in the offset estimation. Therefore, our final estimate of the Seasat and Geosat offset is constant in space. The assessed spatial variability of the offsets is in turn included

in the uncertainty estimate and makes the estimate much more uncertain than for ERS-1/ERS-2/CryoSat-2 LRM. It is legitimate to adapt the offset estimation to what is possible, as long as the uncertainties are adapted accordingly. We clarified this in our explanation of the Geosat/Seasat offset estimation.

Comment 27: P10 L15 – The extrapolation and interpolation steps are not sufficient. It doesn't account for the spatially variable pattern of thinning, which increases towards the coast and is larger on fast flowing ice streams, and the method is not fully described. What is the maximum distance over which gaps are filled? In areas such as the ice sheet edge or on the Antarctic peninsula, which receive exceptionally poor coverage in earlier missions, how are these larger gaps filled? Equally, in order to state EAIS, WAIS, and continent wide thinning rates, the pole hole needs filling.
We explicitly do not perform an extrapolation to unobserved regions (not at the margins and not in the polar gap as well). This was achieved due to the criterion of different sectors around the cell, which need to contain data. Only cells which are surrounded by observations were filled. During the revision of the manuscript, we modified this criterion to be even more strict. In our final grid, now, we calculate a value only for 10x10 km cells that are within a beam-limited radar footprint of repeat altimetry results. A more detailed description has been added to Sect. 3.3.3 and C.4.

The 'Results' and the 'Discussion' section has been completely rewritten, so many of the following comments have been considered but do not apply directly to the revised version.

Comment 28: P10 L31 – The signal in the 1978 to 1992 map is extremely noisy with lots of variation over short spatial scales. Although the authors assert that 'coherent signal' can be obtained from these missions, to me it looks like the differences are as great if not greater than the similarities between the later data. Generate a difference map, or statistics, to quantitatively demonstrate that the results form the early missions are 'coherent', or similar to those from later missions.
We agree that this point should have been explained in more detail. Differences to the results over later periods logically arise due to interannual variations. However, as the whole section has been redesigned, this does not apply to the revised version any more.

Comment 29: P10 L32 – The authors attribute elevation change across the ice sheet to ice dynamics without providing evidence in support of this. Elevation change can be caused by dynamic ice thinning, a snowfall anomaly, change in the scattering horizon, or measurement error, so all of these factors will influence the result not just dynamic thinning alone. Which specific regions are attributed to dynamic change? If based on previous publications, please provide relevant citations. The authors should quantify how much of the elevation change is dynamic, vs all of these other factors, in order to demonstrate that it's the largest contributor.
In the revised version of this section, this very important remark has been taken into consideration carefully.

Comment 30: P10 L33 – State what's classed as a short time scale, annual/ sub-decadal/ other?
This does not apply directly to the revised version any more but has been taken into consideration in the wording.

Comment 31: P11 L1 – Again maps of elevation change are not evidence of change in dynamic thinning without additional supporting data. The authors need to quantify and rule out the influence of snowfall variations, change in scattering horizon, and error, and a corresponding change in ice speed should also be observed. Without this elevation change due to long term, decadal fluctuations in snowfall, may be mischaracterized as dynamic change. The authors should also state which regions they are referring to.
The passage has been rewritten.

Comment 32: P11 Fig5a – Add distance markers to the flow line on one of the maps, hard to tie 5b to locations along it. For example, what distance is the limit of Seasat and Geoset data?
With regard to this and the following comment, this figure has been replaced (now Fig. 9). Both comments would have been very difficult to apply while still keeping the figures readable.

Comment 33: P11 Fig5b – Add error bars to this plot.
See answer above. Figure 9 now contains error bars.

Comment 34: P12 Fig6 – Provide a spatially variable error map for each of these epochs. So far the results have been presented without any error method described, or measurements included in the plots.
Respective maps have been included in the supplement.

Comment 35: P12 L4 – Edit text. The discussions aren't controversial, there is just are just different approaches each of which have advantages and limitations.
Changed.

Comment 36: P13 Fig7 – Add error bars to all lines on this plot.
We added error bars to our altimetry results. Error bars for all data would be hard to identify in the plot.

Comment 37: P13 Fig7 – Clarify how the % coverage has been calculated, and add coverage labeling to an axis. For Antarctica and the LPZ, I don't see how it can be 100during the 1990's when the pole hole is not observed. Additionally, in the methods its stated that the raw data was originally gridded at 1km resolution, which will result in data gaps of several kilometers between tracks before the CryoSat's precessing orbit comes online. So again I struggle to see how such complete observational coverage is achieved, unless extrapolated and interpolated data is classed as an observation, which of course it isn't. Could the authors clarify?

The gridding is described in more detail now. The percentage of coverage serves as ancillary information for the interpretation, only. We think a label is not necessary to see when the coverage was almost 100% and when it was only 80%. Instead, we want to keep the plot itself as large as possible.
Concerning the polar gap: The caption says 'of the Antarctic Ice Sheet north of 81.5°S', which means *excluding the polar gap*.
Concerning the distinction between 'observed' and 'unobserved' we would like to stress that the majority of the 'raw' data in fact has beam-limited footprints of 20 km. We process the data at each kilometer but within overlapping circles of 2 km in the parameter fit. We calculate a value for our final gridded result (with a resolution of 10 km) only if the closest data is less than 20 km away (in the TCD version, the applied criteria to decide, whether we calculate a value or not was different, but the effect was similar). Hence, as we do not extrapolate to regions which are not close (in terms of a footprint) to data, we call our final result 'observed'.

Comment 38: P14 Fig8 - Add error bars to all lines on this plot.
See response above.

Comment 39: P14 Fig8 - Add % coverage axis label to plot. Same comment applies about how the coverage calculation is done.
See response above.

Comment 40: P14 Fig8 – Add a table in the SOM with the areas of the drainage basin sub-regions used to generate this plot.
Done.

Comment 41: P15 Fig9 – I don't understand the figure caption, please rewrite more clearly.
Removed during revision.

Comment 42: P16 L1 to 14 – These results sections are very poorly written as no actual results are described! The authors just state what some of the figures show, and leave the reader to do all the hard work of reading off numbers and key statistics, comparing this with numbers they have read in previous studies. Rewrite the results section to present some actual results. I don't think a single elevation change number has been presented in the text yet, despite that being the title of the paper!
Completely rewritten.

Comment 43: P16 L9 to 13 – The authors have described what this plot is, but haven't explained why it matters or what the key scientific result is. Either remove figure 9 or explain why its an important addition.
This is obsolete now.

Comment 44: P16 F10 – Label y axis of b, presumably count. Edit figure caption to state time period data validated over.
The validation has been completely revised, this is obsolete.

Comment 45: P16 L15 – The validation performed in this paper is completely insufficient, and I would argue it leaves the result presented essentially unvalidated. Use of only 19 GNSS profiles, in a region of no known change, over a limited time period and spatial extent, and on unchallenging flat terrain, does not inform the reader about the validity of these results. At a minimum the authors must use a more comprehensive independent dataset, e.g. ice bridge.
We agree, that a comparison with IceBridge could be interesting and included it.
Nevertheless, we do not think, that the previous validation leaves the results 'essentially unvalidated'. The elevation change is not important here. Our validation analyzes if both data sets see the same elevation change between two epochs. It doesn't matter if this is 1 cm or 20 m. The temporal coverage of IceBridge (2002-2016) is practicably the same as for the GNSS profiles (2001-2015). However, we agree that the coverage of more challenging terrain by IceBridge is also interesting. For this reason, we now validate with both data sets and made our validation now slope dependent.

Comment 46: P17 L2 – This 'validation' cannot be interpreted as an error. A formal error budget based on the altimetry data itself must be documented and added to the plots in this paper. Validation and error estimation are separate things.
Changed.

Comment 47: P17 L14 – The authors don't need to limit their validation data to in situ measurements, much more spatially and temporally extensive airborne data is available and this should be used.
From a satellite point of view, we consider also airborne data as in situ. However, the sentence this comment refers to is about 'the earlier missions'. We would be happy about any suggestions on pre-2000 validation data with more than 'a limited time period and spatial extent'.

Comment 48: P17 L21 – State the number, don't leave the reader to guess how much elevation change you have measured! Presumably it is different for the peninsula and east Antarctica, so again please present your result.
Numbers and some more details added.

Comment 49: P17 L22 – Add figure number.
Location of the reference changed.

Comment 50: P17 L23 – Add figure number, or label somewhere. Location of ice streams mentioned hasn't been identified on any plots in this paper. State quantitatively how your numbers compare with this thinning rates presented by Rignot (2006), the time period is different so there should be something new to say.
The location of the glaciers have been marked in Fig. 10b now. The Rignot (2006) paper uses the input-output method. They map the ice velocity and use these values to obtain ice mass balances. Quantitative numbers for thinning are not given there. Anyways, we added our maximum thinning rates for the respective glaciers to allow for such a comparison in future.

Comment 51: P18 L2 to 6 – Use statistics to show the agreement, or disagreement between the elevation change and precipitation anomaly. State with numbers what 'significant difference' is that allows ice dynamics to be determined. State how far inland the thinning was in earlier decades vs how far inland it reaches now.
This passage is largely edited. We now set the plots to be compared (Fig. 14 now) side by side. We also added a whole section concerning the comparison between SEC from a firn model and from our altimetry data (Sect. 4.2). Correlations for the basin mass time series can be found in F.3. The inland thinning was well reported by Konrad et al. (2016), which is cited here.

Comment 52: P18 L14 – State the threshold used to determine a strong snowfall anomaly. It looks like it varies just as much at different times around other regions in Antarctica.
Obsolete in the revised version.

Comment 53: P18 L15 – what distance away from the grounding line were Seasat and Geosat

typically able to observe.
This strongly depends on the topography, the state of the tracking window loop and the orbit direction. It is now discussed concerning Fig. 9 and can also be seen in Fig. S3.

Comment 54: P18 L20 – The 12 m/yr thinning suggested by Li et al was due to grounding line retreat between '96 and 2013, however the 12 m thinning present in this paper is for 1985 – 2010. Given that the measurements presented in this paper start approximately a decade earlier, if as this paper sats the glacier was already thinning in the 80's then the magnitude and rate are not in agreement with Li et al. Please clarify.
This section has been completely rewritten.

Comment 55: P18 L 23 – The authors need to take more care before attributing elevation change to dynamic ice mass loss. There are many signals present in their continent wide maps that may well not be attributed to dynamic ice loss. There is not consensus in the published literature that all Antarctic peninsula elevation change is dominated by ice dynamics, and the authors themselves later attribute a different elevation change signal on the peninsula to precipitation anomalies without providing any more or less evidence that a different process could be responsible (P18 L30). The authors must present quantitative evidence to support their claims either way.
The wording has been changed to be more precise.

Comment 56: P18 L30 – GRACE data cannot disentangle whether elevation change is caused by snowfall anomaly or ice dynamics, as ice mass is lost in both instances. Only velocity data can demonstrate whether ice was exported from the catchment at an increased rate, proving ice dynamics. Both dynamic thinning and snowfall anomalies result in mass loss, but gravimetry mass loss measurements don't show which of these two different processes might be the cause.
This was a misunderstanding. We were arguing that we see an anomaly and that ERA-Interim sees the same, hence it is very likely a snowfall anomaly. GRACE just confirms the anomaly, not the origin. We changed the wording to be more precise.

Comment 57: P18 L35 – Quantify very well.
Obsolete.

Comment 58: P19 L10 – In Fig S7c I can't see any 2002 step in the precipitation time series so its not clear to me that there is good agreement. Again please provide quantitative stats to back this up, rather than just making unsupported qualitative statements. Cite Lenaerts et al 2013 with respect to the 2009 and 2011 precipitation anomaly results as not a new result from this paper.
Edited.

Comment 59: P19 L16 – While this appears to be true for 2008/10, there is a more significant accumulation gain in the 1990's that is not visible in the elevation change result at all. This is in part because the authors are comparing different things, snow mass anomaly, vs elevation change. Direct comparison not possible unless elevation change converted to mass change.
The volume to mass conversion has been included in the revised manuscript. The respective difference in the 1990's, however, is still present. The correlation in Fig. 8a shows that there are regions where the interannual variation of the FDM and of the altimetry do not agree very well. A more detailed analysis what causes this specific disagreement would be very interesting but is beyond the scope of this paper.

Comment 60: P20 Table2 – There is negligible data coverage outside of East Antarctica prior to 1992, so not valid to include an Antarctic wide number for the '78 to 2017 period in row 3. Remove this number as misleading.
Done.

Comment 61: P21 Conclusions – There are no key results from this paper presented in the conclusions. Add a few key numbers.
Done.

Comment 62: SOM A.1 – State threshold used to determine if noise is too high.
This is a flag, contained in the data from GSFC.

We have listed all the flags and criteria for data editing in a descriptive way (which also applies to the following data). For some of the datasets (as from GSFC), the data does not contain

fixed names. The documentation does only contain a description to the parameters. The ERS data comes with auxiliary files containing additional flags, not included in the binary data files. Furthermore, the ERS data contains outlier in the time tags ('time jumps') as reported by the RA L2 Validation Report. Some of them are flagged but we found several outliers in timing also in the remaining data. All those details are very technical and cannot simply be listed as 'flags and thresholds'. We think the commonly used descriptive text is sufficient as it is done by a range of other publications (Smith et al., 2009; Pritchard et al., 2012; Fricker and Padman, 2012; Sørensen et al., 2015; Paolo et al., 2016) (while many others don't mention data editing at all).

Comment 63: SOM A.1 – State the start and end date for each satellite dataset used.
Very good point. Table added.

Comment 64: SOM A.2 – State which retracker the elevation measurements were derived from.
Our own, see Sect. 2.1.

Comment 65: SOM A.2 – State the specific name of the metadata flag used to filter out data, and if a threshold was used, state the number that this was set at.
See above.

Comment 66: SOM A.2 – Adjust Figure 1 to reflect the actual time period of ERS-1 data used. (same applies for all missions)
Done.

Comment 67: SOM A.3 – State which retracker the elevation measurements were derived from.
Our own, see Sect. 2.1.

Comment 68: SOM A.3 – State specifically which measurement confidence flags were used, and again if a threshold was used, state the number that this was set at.
See above.

Comment 69: SOM A.4 – State specifically which measurement confidence flags were used, and again if a threshold was used, state the number that this was set at.
See above.

Comment 70: SOM A.5 – State which LRM retracker the elevation measurements were derived from.
See above.

Comment 71: SOM A.5 – State specifically which measurement confidence flags were used to filter data, and again if a threshold was used, state the number that this was set at.
See above.

Comment 72: SOM B – Edit title and section text to be more specific as its unclear specifically what the authors have reprocessed? Is it that the elevation measurements have been retracked? Read as a stand alone section I don't know what
The section has been edited accordingly.

Comment 73: SOM E S6 and S7 - Add error bars to all lines on this plot. Add % coverage axis label to plot. Same comment applies about how the coverage calculation is done.
Error bars added to altimetry. Concerning the %-label, we refer to our answer to comment 37.

References

Bamber, J.: Ice Sheet Altimeter Processing Scheme, Int. J. Remote Sensing, 14, 925–938, 1994.

Fricker, H. and Padman, L.: Thirty years of elevation change on Antarctic Peninsula ice shelves from multimission satellite radar altimetry, J. Geophys. Res., 117, https://doi.org/10.1029/2011JC007126, 2012.

Helm, V., Humbert, A., and Miller, H.: Elevation and elevation change of Greenland and Antarctica derived from CryoSat-2, The Cryosphere, 8, 1539–1559, https://doi.org/10.5194/tc-8-1539-2014, 2014.

Kallenberg, B., Tregoning, P., Hoffmann, J., Hawkins, R., Purcell, A., and Allgeyer, S.: A new approach to estimate ice dynamic rates using satellite observations in East Antarctica, The Cryosphere, 11, 1235–1245, https://doi.org/10.5194/tc-11-1235-2017, 2017.

Konrad, H., Gilbert, L., Cornford, S., Payne, A., Hogg, A., Muir, A., and Shepherd, A.: Uneven onset and pace of ice-dynamical imbalance in the Amundsen Sea Embayment, West Antarctica, Geophys. Res. Lett., https://doi.org/10.1002/2016GL070733, 2016.

Paolo, F., Fricker, H., and Padman, L.: Constructing improved decadal records of Antarctic ice shelf height change from multiple satellite radar altimeters, Remote Sens. Environ., 177, 192–205, https://doi.org/10.1016/j.rse.2016.01.026, 2016.

Pritchard, H., Ligtenberg, S., Fricker, H., Vaughan, D., van den Broeke, M., and Padman, L.: Antarctic ice-sheet loss driven by basal melting of ice shelves, Nature, 484, 502–505, https://doi.org/10.1038/nature10968, 2012.

Schröder, L., Richter, A., Fedorov, D., Eberlein, L., Brovkov, E., Popov, S., Knöfel, C., Horwath, M., Dietrich, R., Matveev, A., Scheinert, M., and Lukin, V.: Validation of satellite altimetry by kinematic GNSS in central East Antarctica, The Cryosphere, 11, 1111–1130, https://doi.org/10.5194/tc-11-1111-2017, 2017.

Smith, B., Fricker, H., Joughin, I., and Tulaczyk, S.: An inventory of active subglacial lakes in Antarctica detected by ICESat (2003–2008), J. Glac., 55, 573–595, https://doi.org/10.3189/002214309789470879, 2009.

Sørensen, L., Simonsen, S., Meister, R., Forsberg, R., Levinsen, J., and Flament, T.: Envisat-derived elevation changes of the Greenland ice sheet, and a comparison with ICESat results in the accumulation area, Remote Sens. Environ., 160, 56–62, https://doi.org/10.1016/j.rse.2014.12.022, 2015.

Authors response to the comments of referee #2

We thank referee #2 for the thorough and insightful review of the manuscript. The reviewer criticized a lack of 'well-defined objectives' and 'new insights'. Furthermore, the reviewer argues that the methodology and results should be placed in the context of ice shelf observations of Fricker and Padman (2012) and Paolo et al. (2016), that the discussion of error measures should be included, that besides the kinematic GNSS profiles also IceBridge should be included in the validation and finally, that the volume time series should be converted to mass.

We have put much effort in rewriting the respective sections and think that this contributed to a much clearer presentation of the methodology and the results now. The revised 'Results' section starts with some examples for the surface elevation changes (SEC) at some selected locations, then presents the spatial pattern of the results over different time intervals and finally (after a conversion to mass) provides different time series of basin scale mass changes. The objective of this manuscript is to show which points have to be considered when combining the different satellite altimetry missions, to prove that our approach did successfully deal with these points and to give some examples for the application of the results. As stated in the revised 'Introduction', it is not possible to fully exploit the whole potential of this data set in this paper. Nevertheless, we think that after the revision, the objectives are much clearer now and, also by including significantly more quantitative results, it provides several new insights. The reviewer argues that 'most of the patterns have already been described by other authors'. We think that the point that our measurements see similar patterns and effects as previously reported by other authors (with different data and methods) is not a weakness but, instead, proves the reliability of our results.

To provide further evidence for the successful merging of the data sets, we added the IceBridge data as well as a comparison of the anomalies with a firn model. In order to better discuss this work in the context of previous work, we have completely rewritten the introduction, which now also gives an overview over different previously published approaches to multi-mission altimetry processing.

We totally agree that the inclusion of our uncertainty estimates contains very important information. Hence, we added several maps, error bars and (mainly in the supplement) a detailed description how we obtain these uncertainty estimates.

The reviewer mentions two 'assumptions and simplifications', which might influence the result. The first (1) is the impact of unmodeled effects on our time series. We have added Sect. C.1 to the supplement which discusses our choice of parameters and the impact of these choices. This section, furthermore, contains more detailed information about our outlier detection.
The second (2) is the *stable linear trend* criterion when calibrating Seasat and Geosat. We have revised this criterion. We now introduce additional information about the data gaps between the missions using a firn model. We have shown now that after the offset correction, the anomalies differ by 0.26 ± 0.32 m for Seasat and 0.12 ± 0.31 m for Geosat, which agrees very well within the respective uncertainty.

In the following we will respond to the specific comments one by one.

Comment 1: Throughout the paper the reconstructed changes are described as ice sheet elevation changes. However, changes due to vertical crustal deformations (GIA) have been removed from the reconstructed elevation change rates (page 10, lines 32-34). Therefore, it would be more appropriate to call the parameter ice thickness change.
The mentioned section described how the basin scale ice volume change time series (Fig. 7 and 8 in the TCD manuscript) were generated. Earlier results, which we called 'surface elevation changes (SEC)', were not corrected for GIA. We have changed the structure of the results section, which makes it clearer that the GIA correction was only applied to the 'Ice Sheet mass time series'.

Comment 2: Abbreviations should be spelled out when they appear first, e.g., ESA, SARIn.
We have spelled out SARIn. However, the 'The Cryosphere - English guidelines and house standards' say that abbreviation do not need to be defined when they 'are better known than their written-out form (e.g. NASA, GPS, GIS, MODIS).' In our opinion, this applies to ESA as well.

Comment 3: Page 2, lines 15-16: use release numbers instead of "most recent".

As mentioned at the end of this paragraph, all details, including the release numbers, are located in the supplement. We modified this paragraph, so this information appears directly after the data center listing now.

Comment 4: Page 3, lines 10-11: add beam limited, i.e., approximately 20 km "beam limited" footprint;
Done.

Comment 5: lines 14-18: more details are needed to explain on how to find the POCA
Text edited for easier understanding.

Comment 6: line 24: ICE-1 and ICE-2 methods need to be described;
The description of ICE-1 has been modified for more clarity. A reference for ICE-2 has been added

Comment 7: line 25: remarkably higher precision than what?
Edited.

Comment 8: Page 4, line 22: spell out CFI retracker, include reference.
CFI means 'Customer Furnished Item'. However, the written out form is widely unused. Instead, we added a reference.

Comment 9: Pages 6, 7: it would work better to explain first why the planar surface approximations are different for the different missions, followed by the equations.
Done.

Comment 10: Page 7: outlier detection procedure should be explained in detail.
Explained now in detail in the supplement C.2.

Comment 11: Page 9: explain the use and effect of the moving median filter.
Explained now in detail in the supplement C.3.1.

Comment 12: Page 10, lines 2-4: provide more details on the spatiotemporal smoothing, why was it performed and how effective was it?
Explained now in detail in the supplement C.4.

Comment 13: Line 10: explain the definition of "each month observed". Is there a minimum number of observations or spatial coverage?
Explained in C.4 now as well.

Comment 14: Line 15: how are the surface elevation change rates determined? Are these average rates determined by straight line fitting in temporal domain?
This has been explained in detail now in Sect. 5.1.

Comment 15: Page 16, lines 10-12: the error of the trend (slope of the linear fit) is not the standard deviation from the linear fit and can easily be estimated from the data.
We are not sure how the reviewer defines 'standard deviation from the linear fit'. This was the formal error of the trend parameter obtained by the fit. However, in the revised version we changed the way how we calculate trends. Instead of a fit, we now use the differences between epochs. This is discussed in Sect. 5.1. This also applies to the rates from the time series. The respective uncertainty is discussed in Sect. F.2.

Comment 16: Page 18, line 4-6: the long-term trends over Kamb Ice Stream and Totten Glacier have been detected earlier, for example by Zwally et al., 2015.
For this reason, the sentence continued with 'which was already reported by a range of previous publications (e.g. Wingham et al., 2006; Flament and Rémy, 2012; Helm et al., 2014; Zwally et al., 2015).'

Comment 17: Page 18, lines 29-34: it is not clear what this statement refers to: "Around kilometer 600 where the profile bends into the main flowline of Totten Glacier, we see a significantly rising elevation. The profiles at different epochs reveal that this is not a continuous change but that there is a distinct jump in the early 2000s." Maybe a different representation and a more detailed explanation would help.
The whole paragraph has been completely revised.

Comment 18: Table 1: $\sigma_{constant}$ is a misleading parameter name – σ_{flat} or $\sigma_{noslope}$ might be better.
Changed to σ_{noise}.

Comment 19: Figure caption should include the type of retracker used, i.e., 10%-threshold retracker from this study. Better yet, a comparison of the performance of the different retrackers (from Fig. 2, Fig. S2) could be compared in this table.
Table has been modified accordingly.

Comment 20: Figure 1. The southern extents of the different radar altimetry missions are not clearly presented in the left panel.
Figure + caption modified.

Comment 21: Figure 2. ICE-2 retracker is mentioned in this figure caption only, not in text. Needs more explanation.
Done.

Comment 22: Figure 4. Time axis labels should be fixed. Describe vertical axis. Should show the combined time series.
In the submitted pdf, the time axis was complete. This issue occurred when the journal header was added for the Discussion Paper. The comments concerning the vertical axis and the additional final result have been adapted accordingly.

Comment 23: Figure 5. Define the yearly mean surface elevation change.
This is obsolete as the results have been presented in a entirely different way now.

References

Flament, T. and Rémy, F.: Dynamic thinning of Antarctic glaciers from along-track repeat radar altimetry, J. Glac., 58, 830–840, 2012.

Fricker, H. and Padman, L.: Thirty years of elevation change on Antarctic Peninsula ice shelves from multimission satellite radar altimetry, J. Geophys. Res., 117, https://doi.org/10.1029/2011JC007126, 2012.

Helm, V., Humbert, A., and Miller, H.: Elevation and elevation change of Greenland and Antarctica derived from CryoSat-2, The Cryosphere, 8, 1539–1559, https://doi.org/10.5194/tc-8-1539-2014, 2014.

Paolo, F., Fricker, H., and Padman, L.: Constructing improved decadal records of Antarctic ice shelf height change from multiple satellite radar altimeters, Remote Sens. Environ., 177, 192–205, https://doi.org/10.1016/j.rse.2016.01.026, 2016.

Wingham, D., Shepherd, A., Muir, A., and Marshall, G.: Mass balance of the Antarctic ice sheet, Phil. Trans. R. Soc. Lond. A, 364, 1627–1635, https://doi.org/10.1098/rsta.2006.1792, 2006.

Zwally, H., Li, J., Robbins, J., Saba, J., Yi, D., and Brenner, A.: Mass gains of the Antarctic ice sheet exceed losses, J. Glac., 61, 1019–1936, 2015.

Authors response to the comments of A. Shepherd.

We would like to thank A. Shepherd for the very helpful and insightful comments. We have made a major revision of the manuscript, added a detailed description of our uncertainty estimates, a validation with IceBridge data and converted our final results from volume to mass.

Comment 1: Title. The title is misleading; a minority (25%) of the data set spans 4 decades. It should be modified to explain this or address the majority data set
The title has been modified so it doesn't imply four decades for the 'whole' Ice Sheet any more.

Comment 2: Error budget. The authors use the variance of single cycle crossover differences as a measure of error, and conclude that the reduced variance offered by their preferred retracker indicates a de-facto improvement in error. This is misleading, as their conclusion is entirely related to their choice of error metric and is therefore subjective. To conclude an improvement the authors should evaluate each retracker against independent observations of greater and known precision.
We did this by validating our retracked data as in Schröder et al. (2017). This shows similar improvements. However, as explained in detail in the manuscript, this is a measure for accuracy, not precision. Such a validation imposes systematic errors due to the different sampling of topography, which has to be considered when absolute elevations are important. With respect to elevation change detection, we chose the precision (or 'repeatability') as a measure for uncertainty. This is discussed in Sect. 2.3.

Comment 3: Methods. The authors discuss that a variety of approaches have been used to derive continental scale elevation change measurements, leading to apparently large differences in solutions, and yet they present only one solution. The reader is unable to assess whether the presented solution is optimal. The authors should show how the choice of power correction, firn correction, retracker, elevation change solver, spatial and temporal sampling, spatial and temporal interpolation, and mission cross calibration, influence the final product.
A description for our uncertainty estimates has been added which assesses the uncertainty of the respective data. However, we would like to stress that the method of repeat track parameter fit is well established. The choices we made are based one the results of previous publications as cited at the respective places in the manuscript.

Comment 4: Validation. Great efforts have been made by others to acquire independent elevation change measurements in Antarctica, for example NASA Icebrige. The authors should make use of these measurements to evaluate their satellite product, and their estimated error budget, in support of their claims that it offers improved accuracy and is optimal.
The validation with IceBridge has been included.

Comment 5: Comparison to GRACE and ERA. I don't understand why the authors have compared altimeter volume changes to mass changes and precipitation anomalies derived from GRACE and from ERA Interim. These are not equivalent, and so a side-by-side comparison has no meaning. There is potential value in contrasting these measurements, if they are each worked up to a common unit such as mass, but that requires more work.
The volume-to-mass conversion has been included in the revised version. Instead of ERA, we now use RACMO and the respective FDM.

References

Schröder, L., Richter, A., Fedorov, D., Eberlein, L., Brovkov, E., Popov, S., Knöfel, C., Horwath, M., Dietrich, R., Matveev, A., Scheinert, M., and Lukin, V.: Validation of satellite altimetry by kinematic GNSS in central East Antarctica, The Cryosphere, 11, 1111–1130, https://doi.org/10.5194/tc-11-1111-2017, 2017.

Four decades of Antarctic surface elevation ~~change of the Antarctic Ice Sheet~~ changes from multi-mission satellite altimetry

Ludwig Schröder[1], Martin Horwath[1], Reinhard Dietrich[1], Veit Helm[2], Michiel R. van den Broeke[3], and Stefan R. M. Ligtenberg[3]

[1]Technische Universität Dresden, Institut für Planetare Geodäsie, Dresden, Germany
[2]Alfred Wegener Institute, Helmholtz Centre for Polar and Marine Research, Bremerhaven, Germany
[3]Institute for Marine and Atmospheric Research Utrecht, Utrecht University, Utrecht, The Netherlands

Correspondence: Ludwig Schröder (ludwig.schroeder@tu-dresden.de)

Abstract. ~~We developed an approach for~~ We developed a multi-mission satellite altimetry analysis over the Antarctic Ice Sheet which comprises Seasat, Geosat, ERS-1, ERS-2, Envisat, ICESat and CryoSat-2. ~~In a first step we apply a consistent reprocessing of the radar alitmetry data which improves the measurement precision by up to 50%. We then perform a joint repeat altimetry analysis of all missions. We estimate~~ After a consistent reprocessing and a stepwise calibration of the inter-mission offsets~~by approaches adapted to the temporal overlap or non-overlap and to the similarity or dissimilarity of involved altimetry techniques. Hence, we obtain monthly grids forming a combined surface elevation change time series.Owing to the early missions Seasat and Geosat, the time seriesspan almost four decades from 07~~, we obtain monthly grids of multi-mission surface elevation change (SEC) w.r.t the reference epoch 09/~~1978 to 12/2017 over 25% of the ice sheet area (coastal regions of East Antarctica~~2010. A validation with independent SEC from in situ observations as well as a comparison with a firn model proves that the different missions and ~~the Antarctic Peninsula). Since the launch of ERS-1 79% of the ice sheet area is covered by observations. Over this area, we obtain a negative volume trend of -34±5~~observation modes have been successfully combined to a seamless multi-mission time series. For coastal East Antarctica, even Seasat and Geosat provide reliable information and, hence, allow to analyze four decades of elevation changes. The spatial and temporal resolution of our result allows to identify when and where significant changes in elevation occurred. These time series add detailed information to the evolution of surface elevation in key regions as Pine Island Glacier, Totten Glacier, Dronning Maud Land or Lake Vostok. After applying a density mask, we calculated time series of mass changes and find that the Antarctic Ice Sheet north of 81.5°S lost a total mass of -2068±377 ~~for the more than 25-year period (04/1992–12/2017). These volume losses have significantly accelerated to a rate of -170±11 for 2010–2017. Interannual variations significantly impact decadal volume rates which highlights the importance of the long-term time series. Our time series show a high coincidence with modeled cumulated precipitation anomalies and with satellite gravimetry. This supports the interpretation with respect to snowfall anomalies or dynamic thinning. Moreover, the correlation with cumulated precipitation anomalies back to the Seasat and Geosat periods highlights that the inter-mission offsets were successfully corrected and that the early missions add valuable information.~~ Gt between 1992 and 2017.

1 Introduction

Satellite altimetry allows to observe the surface elevation changes of the Antarctic Ice Sheet with unprecedented precision and resolution (Rémy and Parouty, 2009; Shepherd et al., 2012). Different missions concurrently observed the dynamic thinning of several outlet glaciers in West Antarctica and the relative stability of most regions of the East Antarctic Ice Sheet (e.g. Wingham et al., 2006b . However, when going into detail, some significant differences between the rates obtained from different time intervals become evident. While Wingham et al. (2006b) observed is fundamental for detecting and understanding changes in the Antarctic ice sheet (AIS, Rémy and Parouty, 2009; Shepherd et al., 2018). Since 1992, altimeter missions have revealed dynamic thinning of several outlet glaciers in West Antarctica and have put narrow limits on elevation changes in most parts of East Antarctica. Rates of surface elevation change are not constant in time. Ice flow acceleration has caused dynamic thinning to accelerate (Mouginot et al., 2014; Hogg et al., 2017). Variations in surface mass balance (SMB) and firn compaction rate also cause interannual variations of surface elevation (Horwath et al., 2012; Shepherd et al., 2012; Lenaerts et al., 2013). Consequently, different rates of change have been reported from altimeter missions that cover different time intervals. For example, ERS-1 and ERS-2 data over the interval 1992-2003 revealed negative elevation rates in eastern Dronning Maud Land and Enderby Land (25-60°E) and positive rates in Princess Elizabeth Land (70-100°E) using ERS-1 and ERS-2 (1992-2003), Flament and Rémy (2012) observed a contrary pattern using Envisat ((Wingham et al., 2006b), while Envisat data over the interval 2003-2010). Lenaerts et al. (2013) showed that Dronning Maud Land experienced two extreme snowfall anomalies revealed the opposite pattern (Flament and Rémy, 2012) . Two large snowfall events in 2009 and 2011. Such events can have a strong influence on the calculation of surface elevation change rates. Only an observation time span as long as possible can help to reduce the influence of such events and obtain 2011 have induced stepwise elevation changes in Dronning Maud Land (Lenaerts et al., 2013; Shepherd et al., 2012).

In consequence, results derived from a single mission, or even more so, mean linear rates reported from a single mission, have limited significance in characterizing the long-term evolution of the ice sheet (Wouters et al., 2013). Data from different altimeter missions need to be linked over a time span as long as possible in order to better distinguish and understand the long-term elevation trendevolution and the natural variability of ice sheet volume and mass.

Missions with similar sensor characteristics have successfully been combined were combined e.g. by Wingham et al. (2006b, ERS-1 and ERS-2) or and Li and Davis (2008, ERS-2 and Envisat). However, as demonstrated by Khvorostovsky (2012), the Fricker and Padman (2012) use Seasat, ERS-1, ERS-2 and Envisat to determine elevation changes of Antarctic ice shelves. They apply constant biases, determined over open ocean, to cross-calibrate the missions. In contrast to ocean-based calibration, Zwally et al. (2005) found significant differences for the biases over ice sheets with a distinct spatial pattern (see also Frappart et al., 2016) . Also Khvorostovsky (2012) showed that the correction of inter-mission biases over an ice sheet is not trivial. When including missionswith different sensor characteristics (as ICESat offsets over an ice sheet is not trivial. Therefore, Paolo et al. (2016) cross-calibrated ERS-1, ERS-2 and Envisat on each grid cell, using overlapping epochs, which is very similar to our approach for these missions. Linking different missions becomes even more challenging when different sensor characteristics are concerned, such as ICESat laser altimetry or CryoSat-2 SARIn), a thorough calibration becomes even more importantinterferometric Synthetic Aperture Radar (SARIn) mode, or when the missions do not overlap in time.

Here ~~, we present an approach to combine the different satellite altimetry missions in order to extend the observation time span as long as possible. We create a combined time series of surface elevation change (SEC) that allows to identify rapid changes associated, e. g., to snowfall events as well as long-term changes as e. g. due to changing ice dynamics over nearly four decades.~~ we present an approach to combine seven different satellite altimetry missions over the AIS. By a refined waveform retracking and slope correction of the radar altimetry (RA) data we ensure consistency of the surface elevation measurements and improve their precision by up to 50%. In the following stepwise procedure, we first process the measurements from all missions jointly using the repeat altimetry method. We then form monthly time series for each individual mission data set. Finally, we merge all time series. For this last step, we employ different approaches of inter-mission offset estimation, depending on the temporal overlap or non-overlap of the missions and on the similarity or dissimilarity of their altimeter sensors.

We arrive at consistent and seamless time series of gridded surface elevation differences with respect to a reference epoch (09/2010). They represent three-month temporal averages sampled every month and an effective spatial resolution of about 20 km sampled to a 10 km grid. We evaluate our results and their estimated uncertainties by a comparison with independent in situ data sets, results from satellite gravimetry and results from regional atmospheric climate modeling. We illustrate that these time series of surface elevation change (SEC) allow to study geometry changes and derived mass changes of the AIS in unprecedented detail. For some examples as Pine Island Glacier, Totten Glacier, Shirase Glacier (Dronning Maud Land) and Lake Vostok, we demonstrate the benefits of the long time series. Finally, we calculate ice sheet mass balances from these data for the respectively covered regions. A comparison with independent data indicates a high consistency of the different data sets but reveals also remaining discrepancies.

While this paper gives some examples for new insights obtained from the presented multi-mission altimetry analysis, it can not fully exploit all potential applications. This will be the scope of future work with this data set.

2 Data

2.1 Altimetry data used

We use the ice sheet surface elevation observations from seven satellite altimetry missions: Seasat, Geosat, ERS-1, ERS-2, Envisat, ICESat and CryoSat-2. Figure 1 gives an overview over their temporal and spatial coverage. The data of the two early missions~~Seasat and Geosat~~ , Seasat and Geosat, were obtained from the Radar Ice Altimetry project at Goddard Space Flight Center (GSFC). For ERS-1, ERS-2, Envisat and CryoSat-2 the most recent ESA products were used. For ICESat the final release from the National Snow and Ice Data Center (NSIDC) was ~~employed. The inter-campaign biases between the ICESat laser operation periods were corrected following Schröder et al. (2017). To remove corrupted measurements , we edited each data set in a preprocessing step . Further information concerning the dataset versions used and details about the flags and thresholds applied in the data editing can be found in~~ used. Further details concerning the dataset versions used are given in the supplement. The data editing criteria, applied to remove corrupted measurements in a preprocessing step are explained there as well.

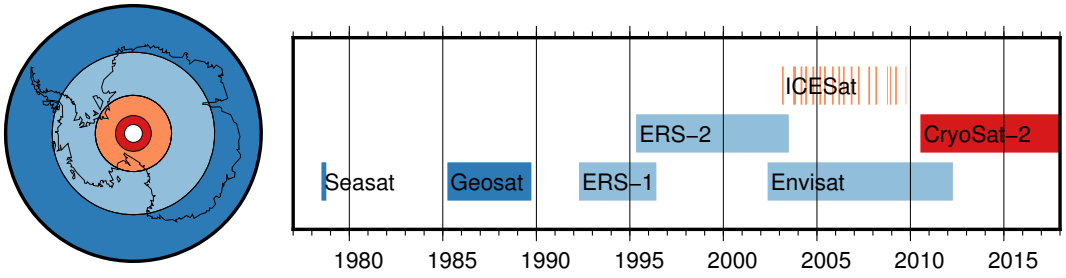

Figure 1. Spatial and temporal coverage of the satellite altimetry ~~missions~~ data used in this study. The colors ~~of the time bars~~ denote the maximum southern extent of the measurements (dark blue: 72°S, light blue: 81.5°S, orange: 86°S, red: 88°S) and thus the size of the respective polar gap.

As illustrated in Fig. 1, due to the inclination of 108°, Seasat and Geosat measurements cover only the coastal regions of the East Antarctic Ice Sheet (EAIS) and the ~~supplementary material.~~ northern tip of the Antarctic Peninsula Ice Sheet (APIS) north of 72°S, which is about 25% of the total ice sheet area. With the launch of ERS-1, the polar gap was reduced to 81.5°S, resulting in a coverage of 79% of the area. The polar gap is even smaller for ICESat (86°S) and CryoSat-2 (88°S), leading to a nearly complete coverage of the AIS in recent epochs.

ERS-1 and ERS-2 measurements were performed in two different modes. ~~With a larger tracking window, the measurements in ice mode are more reliable in coastal areas. Nevertheless, a remarkable amount~~ , distinguished by the width of the tracking time window and the corresponding temporal resolution of the recorded waveform. The ice mode is coarser than the ocean mode, in order to increase the chance of capturing the radar return from rough topographic surfaces (Scott et al., 1994). While the ice mode was employed for the majority of measurements, a significant number of observations has been performed in ocean mode over Antarctica as well (22% for ERS-1, 2% for ERS-2). ~~Hence, we use the data from both modes.~~ We use the data from both modes, as the ocean mode provides a higher precision while the ice mode is more reliable in steep terrain (see Fig. S1 and S3). However, as there is a regionally varying bias between the modes, we treat them as two separate data sets, similar to Paolo et al. (2016).

2.2 Reprocessing of ~~pulse limited~~ radar altimetry

Compared to measurements over the global oceans, pulse limited radar altimetry (PLRA) over ice sheets requires a specific processing to account for the effects of topography and the dielectric properties of the surface (Bamber, 1994). To ensure consistency in the analysis of PLRA measurements, processed and provided by different institutions, we applied our own method for retracking and slope correction.

The slope correction is applied to account for the effect of topography within the ~~beam-limited~~ beam limited footprint (Brenner et al., 1983). Different approaches exist to apply a correction (Bamber, 1994) but it is still a main source of error in ~~radar altimetry~~RA. In Schröder et al. (2017) we showed the clear superiority of the "relocation method", which tries to relate the measurements to the true measurement position, over the "direct method", which determines a correction for the nadir

direction. Roemer et al. (2007) developed a refined relocation method which locates the Point of Closest Approach (POCA) within the approximately 20 km beam limited footprint in a digital elevation model (DEM). We applied this method in our reprocessing chain using the DEM of Helm et al. (2014)based on CryoSat-2. In contrast to the DEM of Bamber et al. (2009) the . The CryoSat-2 measurementshave a , used for this DEM, have a very dense coverage, and hence, very dense coverage and hence, only very little interpolation is necessary, making the DEM spatially very consistent. For the application over the entire continent we optimized this approach further with respect to computational speedlittle interpolation is necessary. Compared to the DEM of Bamber et al. (2009), this significantly improves the spatial consistency. We optimized the approach of Roemer et al. (2007) with respect to computational efficiency for the application over the entire ice sheet. Instead of searching the POCA with the help of a moving window of 2 km (which represents the pulse limited footprint) we applied a Gaussian filter with σ=1 km to the DEM , enabling us to search for the closest point instead of the closest window average. Furthermore, to reach the desired horizontal accuracy, Roemer et al. (2007) use an iterative interpolation approach. Instead, we now estimate the sub-DEM-grid shift component by fitting parabolas to the to resemble the coverage of a pulse limited footprint. Hence, instead of the closest window average, we can simply search for the closest cell in the smoothed grid, which we use as coarse POCA location. In order to achieve a sub-grid POCA location, we fit a biquadratic function to the satellite-to-surface distance within a 3x3 grid cell environment around the coarse POCA grid cell and determine the POCA according to this function.

The retracking of the return signal waveform is another important component in the processing of radar altimetry RA data over ice sheets (Bamber, 1994). Functional fit approaches (e.g. Martin et al., 1983; Davis, 1992; Legrésy et al., 2005; Wingham et al., 2006b) are well established and allow the interpretation of the obtained waveform shape parameters with respect to surface and subsurface characteristics (e.g. Lacroix et al., 2008; Nilsson et al., 2015). However, the alternative approach of threshold retrackers has proven to be more precise in terms of repeatability (Davis, 1997; Schröder et al., 2017). A very robust variant is (Davis, 1997; Nilsson et al., 2016; Schröder et al., 2017). A very robust variant is called ICE-1, using the "Offset Center of Gravity" (OCOG) technique (Wingham et al., 1986), also known as ICE-1amplitude (Wingham et al., 1986). Compared to the waveform maximum, the OCOG-amplitude is significantly less affected by noise . Davis (1997) compared several threshold based results with those of functional fit retrackers and showed that especially low thresholds attain a remarkably higher precision. Following Davis (1997) we (Bamber, 1994). Davis (1997) compared different retrackers and showed that a threshold based retracker, especially with a low threshold as 10%, produces a remarkably higher precision, compared to functional fit based results. We implemented three threshold levels (10%, 20% and 50%) for the OCOG-amplitude to allow an analysis in order to find the optimum thresholdwhich allowed us to analyze the influence of the choice of this level, similar to Davis (1997).

Additionally to PLRA, we also use a reprocessed version of the SARIn mode data from In addition to PLRA, we also use the SARIn mode data of CryoSat-2. The processing is described by Helm et al. (2014), mainly consisting of a refined determination of the interferometric phase and , reprocessed by Helm et al. (2014). The difference with respect to the processing by ESA mainly consisted in a refined determination of the interferometric phase and in the application of a threshold retracker (TFMRA).

2.3 Accuracy and precision

~~The accuracy of radar altimetry derived ice surface elevation measurements has been assessed previously by a crossover comparison with independent data such as the ICESat laser observations (Brenner et al., 2007) or ground based GNSS profiles (Schröder et al., 2017). Such assessments revealed biases which are highly related to the topography. Due to the fact that a pulse limited radar altimeter measures always the POCA, which is the local maximum~~ The accuracy of RA-derived ice surface elevation measurements has been assessed previously by a crossover comparison with independent validation data such as the ICESat laser observations (Brenner et al., 2007), airborne lidar (Nilsson et al., 2016) or ground based GNSS profiles (Schröder et al., 2017). These assessments revealed that with increasingly rough surface topography, the RA measurements show systematically higher elevations than the validation data. This can be explained by the fact that for surfaces that undulate within the ~20 km ~~footprint, but a GNSS-~~ beam-limited footprint, the radar measurements tend to refer to local topographic maxima (the POCA), while the validation data from ground-based GNSS profiles or ICESat-based ~~profile represents the full topography, these differences always include a positive bias over undulating surfaces. Hence, the radar altimetry profiles tend to get biased into positive direction and the standard deviations reach ten meters and more in distinct topography. Nevertheless, this bias does not influence the detection of~~ profiles represent the full topography. Besides these systematic offsets, also the standard deviation of differences between RA data and validation data is influenced by the surface roughness due to the significantly different sampling of the topography. While over flat terrains, most altimeter satellites perform better than 50 cm, in coastal regions the standard deviations can reach ten meters and more. However, both types of error relate to the different sampling of topography of the respective observation techniques. An elevation change, detected from within the same technique, is not influenced by these effects. Hence, with respect to elevation ~~changes from a single mission. Hence, with respect to the detection of elevation changesnot the accuracy but the precision~~ changes, not the accuracy but the precision (i.e. the repeatability) has to be considered.

This precision ~~(i.e. repeatability)~~ can be studied using intra-mission crossovers between ascending and descending profiles. Here, the precision of a single measurement is obtained by ~~dividing the absolute value of the crossover difference between two profiles by $\sqrt{2}$. To rule out significant~~ $\sigma_H = |\Delta H|/\sqrt{2}$ as two profiles contribute to this difference. To reduce the influence of significant real surface elevation changes between the two passes, we consider only crossovers with a time difference of less than 31 days. In stronger inclined topography, the precision of the slope correction dominates the measurement error (Bamber, 1994). Hence, to provide meaningful results, the surface slope needs to be taken into consideration. We calculate the slope from the CryoSat-2 DEM (Helm et al., 2014). The absence of ~~slope related effects on flat terrain allows to study the influence of the retracker~~ slope-related effects on flat terrain allows to study the influence of the retracker (denoted as noise here). With increasing slope, the additional error due to topographic effects can be identified.

~~A comparison of the crossover errors of our reprocessed data with the respective results of the processing versions from the different data centers shows which significant improvements could be achieved by the reprocessingsteps described above (see Fig. 2 for~~

A comparison of the crossover errors of our reprocessed data and of the respective standard products (see supplement for details) shows significant improvements achieved by our reprocessing. Figure 2 shows this comparison for Envisat (similar plots for each data set can be found in the supplement Fig. S1), binned into groups of 0.05° of specific surface slope. The results for

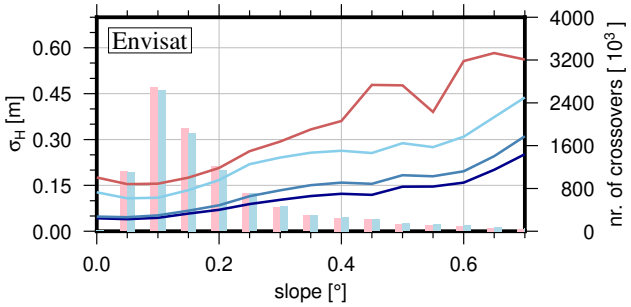

Figure 2. ~~Measurement precision~~ Precision of different processing versions of Envisat measurements from near time (<31 days) crossovers, binned against slope~~($\sigma_H = |\Delta H|/\sqrt{2}$)~~. Red ~~denotes the~~ curve: ESA version with ICE-2 retracker and relocated by mean surface slope. Light, ~~light,~~ medium and dark blue ~~stands for our~~ curves: Data reprocessed ~~data~~ in this study with 50%-, 20%- and 10%-threshold retracker, respectively, relocated using ~~our~~ the refined ~~approach~~method. ~~The~~ Vertical bars~~in the background indicate the~~ : number of crossovers for the ESA (red) and our 10% threshold retracked data (blue)~~data~~.

Table 1. Noise level and slope related component (s in degrees) of the measurement precision, fitted to near time crossovers (unit: m) of the data from the respective data center and our reprocessed data (with a 10% threshold retracker applied).

Data set	Data center	Reprocessed
Seasat	$0.21 + 1.91s^2$	$0.25 + 0.70s^2$
Geosat	$0.17 + 0.86s^2$	$0.18 + 1.16s^2$
ERS-1 (ocean)	$0.25 + 0.90s^2$	$0.09 + 0.18s^2$
ERS-1 (ice)	$0.36 + 2.37s^2$	$0.17 + 0.57s^2$
ERS-2 (ocean)	$0.23 + 0.75s^2$	$0.07 + 0.14s^2$
ERS-2 (ice)	$0.38 + 2.57s^2$	$0.15 + 0.53s^2$
Envisat ~~, similar plots for each dataset can be found in the supplementary material)~~	$0.17 + 1.03s^2$	$0.05 + 0.37s^2$
ICESat	$0.05 + 0.25s^2$	
CryoSat-2 (LRM)	$0.18 + 2.46s^2$	$0.03 + 1.06s^2$
CryoSat-2 (SARIn)	$0.38 + 2.01s^2$	$0.11 + 0.79s^2$

Note that the slope dependent component is weakly determined for data sets with a poor tracking in rugged terrain such as Seasat, Geosat or the ERS ocean mode and for the LRM mode of CryoSat-2.

a flat topography show that a 10% threshold provides the highest precision, confirming the findings of Davis (1997). For ~~each~~ higher slopes, we see that also our refined slope correction contributed to a major improvement. A constant noise level σ_{noise} and a quadratic, slope related term σ_{slope} has been fitted to the respective data according to $\sigma_H = \sigma_{noise} + \sigma_{slope} \cdot s^2$, where s is in the unit of degrees. The results in Tab. 1 show that for each of the PLRA data sets of ~~the PLRA datasets of~~ ERS-1, ERS-2 and Envisat, the ~~crossover error could be reduced by about~~ measurement noise could be reduced by more than 50% compared to ~~ESA's ICE-2 fit~~the ESA product (using the functional fit retracker ICE-2, see Legrésy and Rémy, 1997). With respect to the

CryoSat-2 CFI retracker ~~, the improvement is even larger. With increasing influence of the topography, our refined slope correction shows its superior performance. Also the~~ (Wingham et al., 2006a), the improvement is even larger. Improvements are also significant for the slope-related component. For the example of Envisat and a slope of 1°, the slope-related component is 1.03 m for the ESA product and only 0.37 m for the reprocessed data. The advanced interferometric processing of the SARIn data achieved similar improvements. For the two early missions Seasat and Geosat, the crossover error of our reprocessed profiles is similar to that of the original dataset from GSFC. However, the number of crossover points is significantly increased, especially for Geosat ~~.~~ (see Fig. S1). This means that our reprocessing obtained reliable data where the GSFC processor already rejected the measurements.

~~Besides the noiseof the measurements~~In addition to measurement noise, reflected in the crossover differences, a consistent pattern of offsets between ascending and descending tracks has been observed previously ~~(Legrésy et al., 1999; Arthern et al., 2001)~~ (A-D bias, Legrésy et al., 1999; Arthern et al., 2001). Legrésy et al. (1999) interpret this pattern as an effect of the interaction of the linearly polarized radar signal with wind-induced surface structures~~. Arthern et al. (2001) attribute the differences to anisotropy within the snowpack. Armitage et al. (2014) developed a simple model using the orbit direction of CryoSat-2 and a mean wind field which remarkably resembles the spatial pattern of the bias. McMillan et al. (2014) and also Simonsen and Sørensen (2017) estimate an orbit direction related parameter in their repeat track processing to remove this effect, while Helm et al. (2014) showed , that a low threshold retracker significantly reduces the ascending-descending~~ , while Arthern et al. (2001) attribute the differences to anisotropy within the snowpack. Helm et al. (2014) showed that a low threshold retracker significantly reduces the A-D bias. We observe a similar major reduction (from ±1 m in some regions for a functional fit retracker to ~~less than a decimeter~~ ±15 cm when using a 10% threshold, see Fig. ~~S1 in the supplements). Since, moreover, the final results are smoothed over several kilometers and thus usually contain ascending and descending satellite tracks alike, we conclude that this bias has no discernible effect on our results.~~

~~Constant and slope related component of the measurement precision from near time crossovers. Note that the slope dependent component is weakly determined for datasets with a poor tracking ability of rugged terrain such as Seasat, Geosat or the ERS ocean mode. Data set σ_{const} mσ_{slope} mSeasat 0.25 0.70 Geosat 0.18 1.16 ERS-1 (ocean) 0.09 0.18 ERS-1 (ice) 0.17 0.57 ERS-2 (ocean) 0.07 0.14 ERS-2 (ice) 0.15 0.53 Envisat 0.05 0.37 ICESat 0.05 0.25 CryoSat-2 (LRM) 0.03 1.06 CryoSat-2 (SIN) 0.11 0.79~~

~~The crossover comparison is not only performed for quality control of our processing chain, we also use the results to adequately set weights when combining measurements from different missions in a certain location in the repeat altimetry fit. Therefore we bin the single profile crossover errors ($|\Delta h|/\sqrt{2}$) into 20 groups of specific surface slope and fit a constant plus a quadratic, slope related term to the bin medians ($\sigma_{meas} = \sigma_{const} + \sigma_{slope} slope[^\circ]^2$). Table **??** shows the specific slope related errors of the different data sets. The larger slope dependent component of PLRA data, compared to ICESat, leads to stronger weights of the small footprint measurements of ICESat in regions with a more distinctive topography. Instead, over the flat interior of East Antarctica, the weights are quite similar~~S2). The remaining bias is not larger, in its order of magnitude, than the respective noise. Moreover, near the ice sheet margins, the determination of meaningful A-D biases is complicated

by the broad statistical distribution of A-D differences and the difficulty to discriminate outliers. We therefore do not apply a systematic A-D bias as a correction but rather include its effect in the uncertainty estimate of our final result.

3 Multi-mission ~~analysisSurface elevation change~~ SEC time series

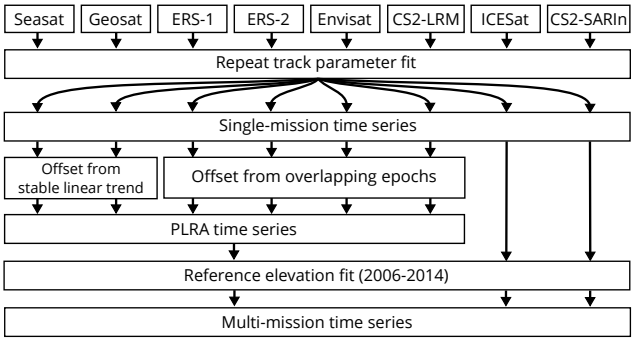

Figure 3. Schematic diagram of the processing steps from the combined repeat track parameter fit over single-mission time series towards a combined multi-mission time series.

3.1 Repeat track parameter fit

We obtain elevation time series following the repeat ~~altimetry~~ track approach, similar to Legrésy et al. (2006) and Flament and Rémy (2012). As the orbits of the missions used here have different repeat track patterns, instead of along-track boxes we perform our fit on a regular grid with 1 km spacing (as in Helm et al., 2014)~~, instead of along-track boxes~~. For each grid cell we analyze all elevation measurements h_i within a radius of 1 km around the grid cell center. ~~As specified in Eq. 1, we fit a linear trend (dh/dt), a plane (a_0, a_1, a_2) and a regression coefficient (dBS) for the anomaly of backscattered power ($bs_i - \overline{bs}$). The search radius of 1~~ This size seems reasonable as for a usual along track spacing of about 350 m for PLRA (Rémy and Parouty, 2009), each track will have up to 5 measurements within the radius. Due to the size of the pulse limited footprint a smaller search radius would contain only PLRA measurements with very redundant topographic information and thus would not be suitable to fit a reliable correction for the topography. As specified in Eq. (1), the parameters contain a linear trend (dh/dt), a planar topography (a_0, a_1, a_2) and a regression coefficient (dBS) for the anomaly of backscattered power ($bs_i - \overline{bs}$) to account for variations in the penetration depth of the radar signal.

For a single mission, the parameters are adjusted according to the model

$$\begin{aligned} h_i = \quad & dh/dt(t_i - t_0) + \\ & a_0 + a_1 x_i + a_2 y_i + \\ & dBS(bs_i - \overline{bs}) + \\ & res_i \end{aligned} \tag{1}$$

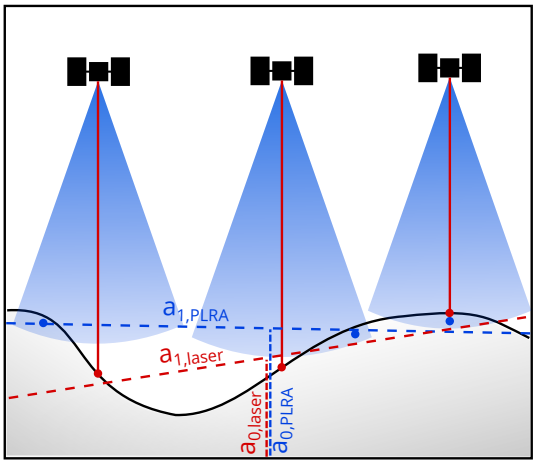

Figure 4. Illustration of the technique-dependent topographic sampling. The laser (red) measures the surface elevation in the nadir of the instrument while for radar altimetry (blue), the first return signal originates from the POCA (marked by the blue point). Hence, ~~the~~ planar surface ~~fitted~~ approximations to the ~~measurements~~ measured heights (dashed lines) ~~should not be mixed over~~ are intrinsically different for the different techniques.

Here, t_i denotes the time of the observation. The reference epoch t_0 is set to 09/2010. x_i and y_i are the Polar Stereographic coordinates of the measurement location, reduced by the coordinates of the cell's center. The residual res_i describes the misfit between the observation and the estimated parameters.

~~For the combined processing of different missions and different altimeter techniques, some of the parameters may vary between the datasets. Thus, they are estimated individually for the respective mission $M(i)$ or observation technique $T(i)$ of the measurement h_i. Hence, the general relation for a combined processing can be expressed as~~

$$\begin{aligned} h_i = \quad & dh/dt(t_i - t_0) + \\ & a_{0,M(i)} + a_{1,T(i)} x_i + a_{2,T(i)} y_i + \\ & dBS_{M(i)} (bs_i - \overline{bs_{M(i)}}) + \\ & res_i \end{aligned}$$

In contrast to this single mission approach, here we perform a combined processing of all data from different missions and even different altimeter techniques. Thus, some of the parameters may vary between the data sets. To allow for offsets between the missions, the elevation at the cell center a_0 is fitted for each mission ~~$M(i)$ individually. The same is applied~~ individually. The same applies to dBS, which might relate to specific characteristics of a mission as well. For Seasat, covering less than 100 days, this parameter is not estimated, as we assume that during the mission life time no significant changes occurred. ~~The same applies to ICESat, where signal penetration is negligible~~ For ICESat, dBS is not estimated either, as signal penetration is negligible for the laser measurements.

Between different observation techniques (i.e. PLRA, SARIn and laser altimetry), also the effective surface slope may differ. Considering the specific footprint sizes and shapes, the topography is sampled in a completely different way as illustrated in Fig. 4. While PLRA refers to the closest location anywhere within the ~20 km beam-limited footprint (i.e. the POCA), CryoSat's SARIn measurement can be attributed within the ~~very narrow Doppler stripe in across track~~ narrow Doppler stripe in cross-track direction. For ICESat the ~70 m laser spot allows a much better sampling of local depressions~~too~~. Hence, the slope parameters a_1 and a_2 are estimated for each of the techniques ~~$T(i)$ independently. This setting allows to fit dh/dt from all missions while still considering the individual peculiarities of each sensor. Also in~~ independently.

Considering these sensor-specific differences, the model for the least squares adjustment in Eq. (1) is extended for multi-mission processing

$$\begin{aligned} h_i = \quad & dh/dt(t_i - t_0) + \\ & a_{0,M(i)} + a_{1,T(i)} x_i + a_{2,T(i)} y_i + \\ & dBS_{M(i)}(bs_i - \overline{bs_{M(i)}}) + \\ & res_i \end{aligned} \tag{2}$$

where $M(i)$ and $T(i)$ denote to which mission or technique, respectively, the measurement h_i belongs.

We define a priori weights for the measurements h_i based on the precision of the respective mission and mode from crossover analysis (Tab. 1) and depending on the surface slope at the ~~weighting of the observations we consider their different characteristics. Using the sensor-specific precision (Tab~~measurement location. This means that in regions with a more distinctive topography, ICESat measurements (with a comparatively low slope-dependent error component) will obtain stronger weights, compared to PLRA as Envisat. In contrast, over flat regions as on the East Antarctic plateau, the weights are very similar. ~~??) we set the weights according to the surface slope at the respective measurements location. Outliers are removed iteratively in the processing. Therefore, we exclude observations where the standardized residuals exceed a value of 5 and repeat the processing until no more outliers are found.~~

~~After fitting all~~

3.2 Single-mission time series

After fitting all parameters according to the multi-mission model (Eq. 2), we regain elevation time series by recombining the parameters ~~according to Eq~~a_0 and dh/dh with monthly averages of the residuals ($\overline{res}$). ~~2, we can regain elevation time series by recombining the parameters with the residuals. We use monthly averages of the residuals , which typically represent the misfit of a single satellite pass towards all respective parameters.~~ For each month j and each mission M, the time series is constructed as

$$h_{j,M} = a_{0,M} + dh/dt(t_j - t_0) + \overline{res_{j,M}}. \tag{3}$$

~~These time series refer to the center of the cell and are corrected for backscatter related penetrationeffects. A schematic illustration of the results of this step is given in Fig. 5a.~~ The elevations $h_{j,M}$ all relate to the cells center and are corrected for

time-variable penetration, as the parameters of the topography slope and backscatter correction are omitted in this recombination. Due to the reference elevation $a_{0,M}$, which also contains the inter-mission offsets, this results in individual time series for each single mission. A schematic illustration of the results of this step is given in Fig. 5a. The temporal resolution of these time series is defined by using monthly averages. These $\overline{res}$ represent the anomalies of typically a single satellite pass towards all respective parameters including the linear rate of elevation change. The standard deviation of the residuals in these monthly averages are used as uncertainty measure for $h_{j,M}$ (see C.2 for further details).

3.3 ~~Merging different missions and techniques~~Combination of the single-mission time series

In order to merge data from different missions into a joint time series, inter-mission offsets have to be determined and eliminated. In the ERS reprocessing project (Brockley et al., 2017), mean offsets between the ERS missions and Envisat have been determined and applied to the elevation data. However, for ice sheet studies inter-satellite offsets are found to be regionally varying ~~(Zwally et al., 2005; Khvorostovsky, 2012)~~(Zwally et al., 2005; Thomas et al., 2008; Khvorostovsky, 2012). When merging data from different observation techniques (PLRA, SARIn and laser) the calibration gets even more challenging.

~~We chose an approach in different steps which is depicted in Fig.5. In a first step, we merge all the PLRA data. For these missions the topographic sampling of~~ We chose an approach in different steps which is depicted in Figs. 3 and 5. Further details concerning the processing of each step can be found in the supplement.

3.3.1 Merging PLRA time series

In a first step, we merge the PLRA time series. For these missions the topographic sampling by the instruments is similar and thus the offsets are valid over larger regions. For overlapping missions (ERS-1, ERS-2, Envisat, CryoSat-2 LRM) the offsets are calculated from simultaneous epochs (~~red area in Fig.5b). Outliers in the regional varying offsets were removed using a moving median filter and the result is smoothed using a gaussian filter (σ = 20). Maps of the offsets with respect to Envisat are shown in the supplementary material Fig. S3.~~ blue area in Fig. 5b), as performed by Wingham et al. (1998) or Paolo et al. (2016). Smoothed grids of these offsets are generated (see Fig. S4) and applied to the respective missions. For the ERS missions, we find significant differences in the offsets for ice and ocean mode, hence, we determine separate offsets for each mode. ~~The~~ Comparing our maps with similar maps of offsets between ERS-2 (ice mode) ~~–Envisat offset distribution looks very similar to the pattern presented by Frappart et al. (2016)~~ and Envisat shown by Frappart et al. (2016) reveals that the spatial pattern agrees very well but we find significantly smaller amplitudes. We interpret this as a reduced influence of volume scattering due to our low retracking threshold. In accordance with Zwally et al. (2005), we did not find an appropriate functional relationship between the offset and the waveform parameters.

To calibrate Geosat and Seasat, ~~which do not have an overlap with other missions, we used the parameter $a_{0,M}$ from Eq. (2). In Fig. 5b the joint trend estimation is depicted by the equal slope of the dashed red lines . The different~~ a gap of several years without observations has to be bridged. As depicted by the dashed blue lines in Fig. 5b, we do this using the trend corrected reference elevations $a_{0,M}$ ~~at t_0 = 09/2010 relate to the calibration offsets. This method, however, is only valid if the rate of~~

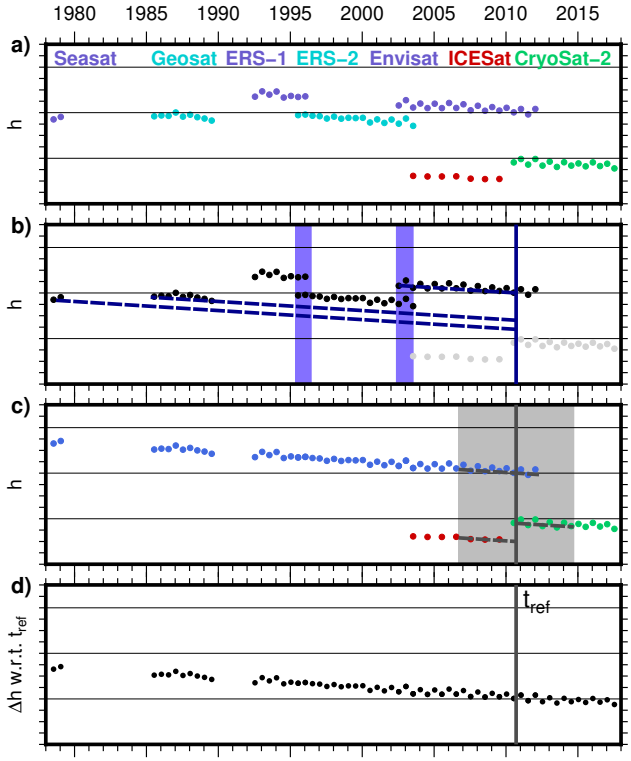

Figure 5. Schematic ~~elevation time series as obtained from Eq. (3) to illustrate~~ illustration of the combination of the ~~different data sets~~missions. **a)** Single-mission time series ~~with inter-mission offsets. To emphasize the different techniques, pulse-limited radar altimetry (~~of PLRA ~~) observations are colored in red~~ missions (blue and ~~pink~~cyan), ~~data from~~ CryoSar-2 in SARIn mode ~~of CryoSat-2 in blue~~ (green) and the laser altimetry measurements of ICESat ~~in cyan~~(red) with inter-mission offsets. **b)** ~~To combine~~ Offsets between the PLRA data ~~,~~ are determined from overlapping epochs ~~are used where they exist~~ (~~ERS1-ERS2, ERS2-Envisat; red~~ blue area) ~~. Otherwise, the offset with respect to the reference mission (Envisat) is obtained from the differences in the surface~~ or trend-corrected elevation ~~parameter a_0 of the fit~~ differences (according to Eq.~~(~~2) ~~(dashed dark red lines; Seasat and Geosat). This~~ where dh/dt is ~~only applicable if all missions show a consistent rate of dh/dt as it is shown here~~sufficiently stable. **c)** The specific offset between PLRA, SARIn and laser data depends on the sampling of the topography within each single cell. ~~Nevertheless, the~~ These different techniques ~~can be combined~~ are aligned by reducing each elevation time series by the specific elevation at the reference epoch ~~(09/2010)~~t_{ref}. ~~To reduce the influence of~~ Due to possible non-linear surface elevation changes, this reference elevation is obtained from a 8-year interval only (gray area). **d)** The combined multi-mission time series contains SECs with respect to t_{ref}.

~~elevation change is sufficiently stable . To find regions where we can assume such a stable rate, we compared the multi-mission~~ from the joint fit in Eq. (2). This, however, can only be done if the rate is sufficiently stable over the whole period. Therefore, we use two criteria. First, we check the standard deviation of the fit of dh/dt~~from Eq. (2) with those, obtained from similar single-mission fits (Eq. 1) for ERS-1, ERS-2, Envisat and CryoSat-2 respectively. Only where all the differences between the single-mission rates and the combined rate are smaller than 5 , we consider the disturbances due to interannual variations~~

or an acceleration of the rate as not significant. Maps of these offsets with respect to Envisat are shown in the supplementary material Fig. S4. This $\sigma_{db/dt}$ indicates the consistency of the observations towards a linear rate during the observational period. However, anomalies during the temporal gaps between the missions (i.e. 1978-1985 and 1989-1992) cannot be detected in this way. Therefore, we furthermore utilize a firn densification model (FDM, Ligtenberg et al., 2011; van Wessem et al., 2018) . This model describes the anomalies in elevation due to atmospheric processes against the long-term mean. The RMS of the FDM time series is hence a good measure for the magnitude of the non-linear variations in surface elevation. Consequently, only cells where $\sigma_{db/dt} < 1\,\mathrm{cm/yr}$ and $RMS_{FDM} < 20\,\mathrm{cm}$, indicating a highly linear rate, are used to calibrate the two historic missions. Maps of the offsets with respect to Envisat are shown in the supplement Fig. S5. Regions where this stability criterion is fulfilled are mainly found on the plateau. The mean values over all cells amount to -0.85amounts to -0.86 m for Seasat and -0.72-0.73 m for Geosat. The corresponding standard deviations of 0.510.85 m and 0.340.61 m respectively are mainly a result of the regional pattern of the offsets. However, here we do not apply a regionally varying offset as we have no information how the offsets could be extrapolated towards the coastal regions where the stability criterionis not fulfilled. Furthermore, parts of the pattern might be explained by SEC anomalies prior to 1992 while afterwards the rate was sufficiently stable. Hence, applying the mean bias is The true offsets are likely to have spatial variations. However, we are not able to distinguish spatial variations of the offset from residual effects of temporal height variations in the regions meeting the stability criterion. In the regions not meeting this criterion, we are not able to estimate the spatial variations of the offset at all. Therefore, our final estimate of the offset, applied to the most robust solution. Within its error bars, it agrees very well with the ocean/sea ice based measurements, is a constant, calculated as the average offset over the regions meeting the stability criterion. The spatial variability not accounted for by the applied offset is included, instead, in the assessed uncertainty. Our bias between Seasat and Envisat (-0.86±0.85 m) agrees within uncertainties with the ocean-based bias of -0.77 m between Seasat and Envisat (Fricker and Padman, 2012). With the help of these biases, all PLRA missions were corrected towards the chosen reference mission Envisatand thus form a joint PLRA time series (red in Fig.used by Fricker and Padman (2012). However, we prefer this offset as the observed medium plays an important role for these biases (see Sect. C.3.2 for a more detailed discussion).

With the help of these offsets, all PLRA missions were corrected towards the chosen reference mission Envisat. Uncertainty estimates of the offsets are applied to the respective time series to account for the additional uncertainty. Hence, the PLRA time series are combined (blue in Fig. 5c with additional CryoSat-2 LRM mode where available). At epochs when more than one data set exists, we apply weighted averaging using the uncertainty estimates.

To determine the biases of CryoSat's SARIn modeand ICESatcompared to PRLA, simultaneously observed epochs could be used again. However, as noted in Sect.3.1 and Fig. 4, the different sampling of topography by the three techniques might lead to completely different surfaces , fitted to the respective elevation measurements . In Eq. (2), this is accounted for by technique specific slope parameters but also the reference elevation ($a_{0,M}$) contains a component of the difference of the effective topography. Hence, the biases between different techniques refer to the effective topographies fitted to the measurements only and are distinct for every grid cell . Only cells which contain measurements from different techniques would hence allow to estimate the bias for this cell. Due to different orbit inclinations, this applies only to very few cells and consequently, the use of individual biases from simultaneous epochs is not satisfactory.

~~Instead, we applied another linear fit to the three, technique specific SEC time series from SARIn, laser and the merged PLRA time series . We estimate a joint dh/dt and an individual reference~~

3.3.2 Technique-specific surface elevation changes

In contrast to the PLRA data in the previous step, when merging data from different observation techniques as CryoSat's SARIn mode, ICESat's laser observations and PLRA, also the different sampling of topography has to be considered. As noted in Sect. 3.1 this might lead to completely different surfaces fitted to the respective elevation ~~$a_{0,T}$ for each technique T for the epoch 09/2010. As unmodelled effects like interannual variations or accelerations in the rate might adulterate~~ measurements and thus, the ~~parameters, we restrict this fit to a short~~ time series need to be calibrated for each cell individually. However, not all cells have valid observations of each data set. Therefore, instead of calibrating the techniques against each other, we reduce each time series by their respective elevation at a common reference epoch and hence obtain time series of surface elevation changes (SEC) w.r.t. this reference epoch instead of absolute elevation time series.

We chose September 2010 as the reference epoch. This epoch is covered by the observational periods of PLRA and CryoSat SARIn and also is exactly one year after the last observations of ICESat, which reduces the influence of an annual cycle. As discussed in Sect. 3.3.1, non-linear elevation changes will adulterate a_0 from Eq. (2), obtained over the full time span. Therefore, we applied another linear fit to a limited time interval of 8 years only (09/2006-09/2014, gray area in Fig.~~5c) which contains all techniques. The~~ 5c). We subtract the variation of the FDM over this period to account for short-term variations. The limited time interval reduces the influence of changes in ice dynamics. We estimate the individual reference elevations $a_{0,T}$ for each technique T and a joint dh/dt. After subtracting the technique-specific reference elevations $a_{0,T}$ ~~are subtracted from the respective time seriesand hence, all series of elevation differences~~ from the respective time series, they all refer to 09/2010 and can be combined. ~~This final combination of the techniques is performed~~

3.3.3 Merging different techniques

We perform the final combination of the techniques using a weighted spatio-temporal averaging with ~~20~~10 km σ gaussian weights in spatial domain ~~and including the two consecutive epochs in the temporal domain to reduce the noise of a single pass. This averaging is used to interpolate unobserved cells as well. Due to the smoothing of the weighting function, we reduce our spatial grid resolution to 10x10~~(up to a radius of 3σ =30 km~~now and did not interpolate a value to cells which are mainly covered by rocks (Burton-Johnson et al., 2016). To avoid extensive extrapolation to unobserved regions, the data around each cells center was classified into six sectors and interpolation was only performed if at least three of the sectors contained data.~~) and over 3 epochs (i.e. including the two consecutive epochs) in the temporal domain. Hence, we obtain grids of surface elevation change (SEC) with respect to 09/2010 for each month observed. Due to the smoothing of the weighting function, we reduce our spatial SEC grid resolution to 10 x 10 km. The respective uncertainties are calculated according to the error propagation. To avoid extrapolation and to limit this merging step to the observed area only, we calculate a value for the respective epoch in the 10 x 10 km grid cells only if we have data within 20 km around the cells center (which is about the size of a beam-limited radar footprint). The five examples in Fig. 6 demonstrate the spatio-temporal coverage of the resulting

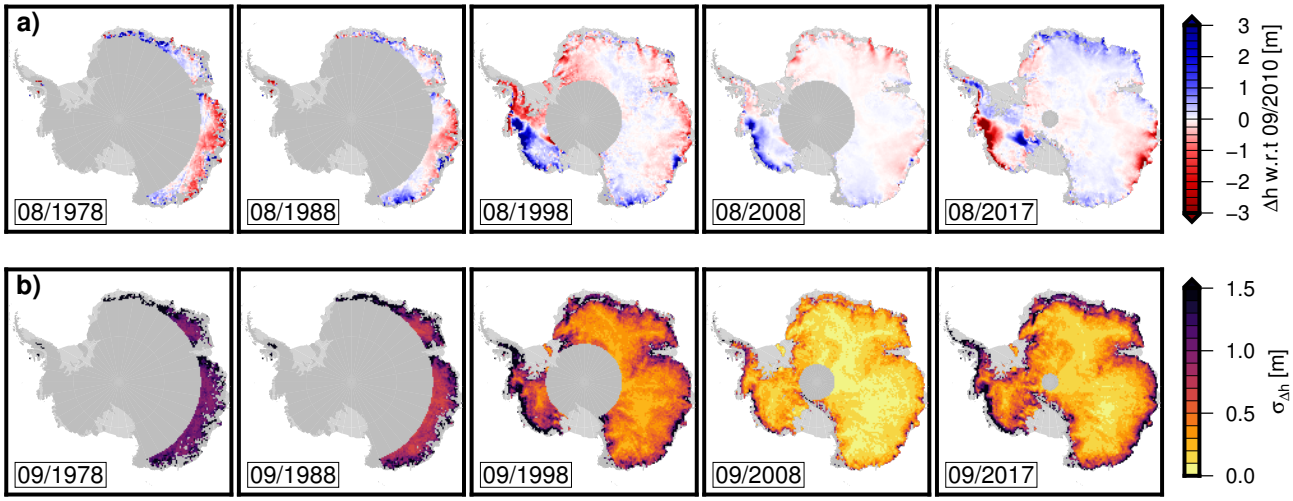

Figure 6. ~~a)~~ Five example snapshots of the resulting combined surface elevation time series (**a**) and their respective uncertainty (**b**). The height differences refer to our reference epoch 09/2010.~~b) Yearly means of surface elevation change along the profile marked by the black line in a) from Totten Glacier towards Lake Vostok.~~

SEC grids at different epochs. The respective uncertainty estimates, given in Fig. 6b (further details in the supplement) reach values of one meter and more. Especially in the coastal regions, these uncertainty estimates of our SECs are not defined by the measurement noise and the uncertainty of the offset alone. In regions with fast elevation changes and a large spatial variation in the signal (such as the flow lines of outlet glaciers), the $\sigma_{\Delta h}$ also comprises the variation of the Δh within the area used for smoothing. This holds especially true for epochs that are far away from the reference epoch and, hence, have large values of Δh. Consequently, the epoch 09/2008 provides the lowest uncertainty estimate in these examples, even lower than the CryoSat-2 based epoch 09/2017.

4 ~~Results~~

~~We obtain grids of surface elevation change (SEC) with respect to 09~~

4 Comparison of SEC with independent data

4.1 In situ observations

To validate our results, we used inter-profile crossover differences of 19 kinematic GNSS profiles (Schröder et al., 2017) and elevation differences from Operation IceBridge (OIB ATM L4, Studinger, 2014). The GNSS profiles have been observed between 2001 and 2015 and most of them cover more than 1000 km. One profile (K08C) has not been used as the poorly determined antenna height offset might impose larger errors. For each crossover difference between kinematic profiles from

different years, we compare the differences of the respective altimetric SEC epochs in this location ($\delta\Delta h = \Delta h_{KIN} - \Delta h_{ALT}$). The same analysis has been performed with the elevation changes from OIB. The flights, carried out between 2002 and 2016, were strongly concentrated along the outlet glaciers of West Antarctica and the Antarctic Peninsula. Hence, they cover much more rugged terrain which is more challenging for satellite altimetry. Nevertheless, over the tributaries of the Amundsen Sea glaciers and along the polar gap of ICESat, some repeated measurements have also been performed over flat terrain.

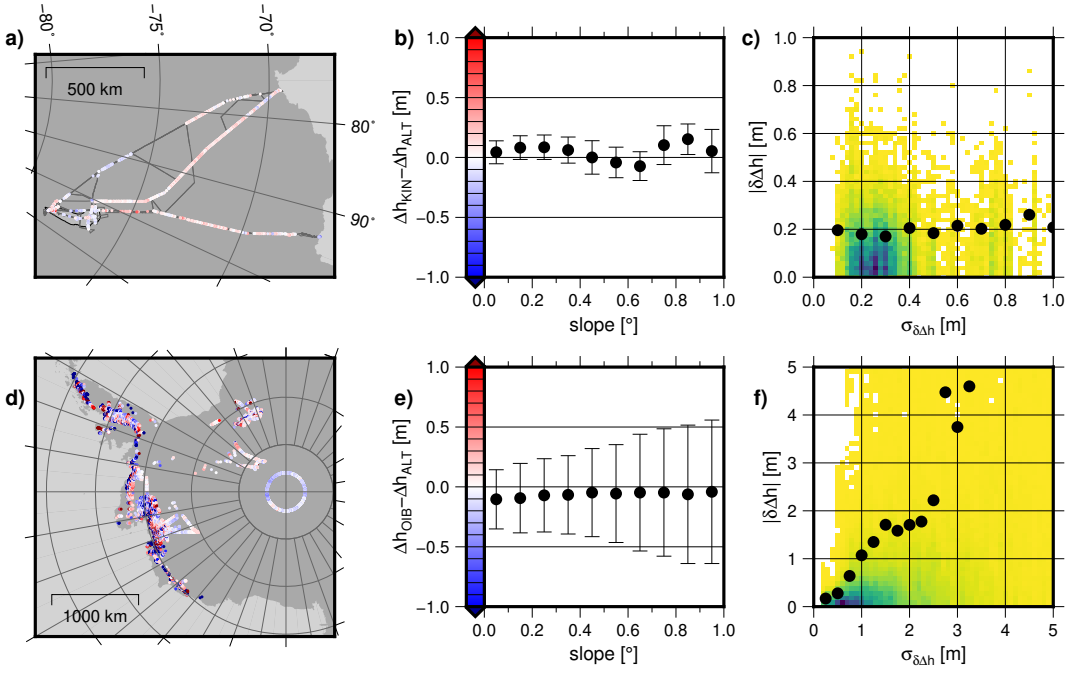

Figure 7. Validation with elevation differences observed by kinematic GNSS (**a,b,c**) and Operation IceBridge (**d,e,f**). Differences between elevation changes observed by the validation data and altimetry are shown on the maps (**a,d**). Median and MAD of these differences, binned by different surface slope, are shown in the center (**b,e**). The right diagrams (**c,f**) show the comparison of these differences with the respective uncertainty estimate, obtained from both data sets. The point density is plotted from yellow to blue and the black dots show the root mean square, binned against the estimated uncertainty.

Figures 7a and d show the results of this validation. A satellite calibration error would lead to systematic biases between the observed elevation differences if Δh_{ALT} is obtained from data of two different missions. However, such biases may also be caused by systematic errors in the validation data. Furthermore, in contrast to the calibration data, the RA measurements may systematically miss out regions which are changing most rapidly if they are located in a local depression (Thomas et al., 2008). With an overall median difference of 6±10 cm for the GNSS profiles and -9±42 cm for OIB, however, the observed elevation changes show only moderate systematic effects and agree within their error bars. The median absolute deviation (MAD) for different specific surface slopes (Fig. 7b and e) reveal the influence of topography in this validation. The GNSS profiles show only a very small increase of this variation with slope. The IceBridge data covers the margins of many West Antarctic glaciers,

where elevation changes differ over relatively short distances. Hence, it is not surprising that we see a significantly larger spread of $\delta\Delta h$ at higher slopes here. However, also for the flat interior, the MAD of the differences is still at a level of 25 cm, which is significantly larger than in the comparison with the GNSS profiles.

The observed $\delta\Delta h$ can further be used to evaluate the uncertainty estimate of the respective elevation differences. In Fig. 7c and f, the uncertainty estimates of the four contributing data are combined and compared to the observed differences. The comparison with both datasets shows that these estimates seem reasonable. In the comparison with the GNSS profiles, the relatively low differences, even in regions which imply a higher uncertainty, are likely just incidental for the small sample of $\delta\Delta h$ along the GNSS profiles.

In conclusion, this validation shows that remaining systematic biases (originating from satellite altimetry or the validation data) are on a centimeter level only and that our uncertainty estimate is realistic. However, we have to stress that only altimetric SEC within the interval 2001-2016 can be validated in this way. For the earlier missions, no spatially extensive high precision in situ data are available to us.

4.2 Firn model

Another data set which covers almost the identical spatial and temporal range as the altimetric data is the firn thickness data set of the IMAU Firn Densification Model (FDM Ligtenberg et al., 2011), forced at the upper boundary by accumulation and temperature of the Regional Atmospheric Climate Model, version 2.3p2 (van Wessem et al., 2018). Before we can compare this model to our SEC results, however, it is important to mention that the FDM only contains elevation anomalies. A long-term elevation trend over 1979-2016, e.g. due to changes in precipitation on longer time scales (Thomas et al., 2015) would not be included in the model. Furthermore, due to the nature of the model, it cannot give information about ice dynamic thinning/~~2010 for each month observed~~ thickening. Hence, to compare the FDM and the SEC from altimetry, we first remove a linear trend. This is performed for the period 1992-2016. The trends are only calculated from epochs where both data sets have data, i.e. in the polar gap this comparison is limited to 2003-2016 or 2010-2016, depending on the first altimetry mission providing data here. After the detrending, the anomalies are used to calculate correlation coefficients for each cell, depicted in Fig. 8a. Figure 8b shows the RMS of these anomalies from the altimetry data, representing the magnitude of the seasonal and interannual variations. Comparing the two maps shows that the correlation is around 0.5 or higher, except in regions where the magnitude of the anomalies is small, i.e. where the signal-to-noise ratio of the altimetric data is low. This relationship is depicted in Fig. 8c, where we see that for the vast majority of cells the correlation is positive. For anomalies with a RMS>0.5 m, the average correlation is between 0.3 and ~~at a 10~~0.6.

Anomalies against the simultaneously observed long-term trend (1992-2016) can also be computed for earlier epochs. Assuming no significant changes in ice dynamics here, these anomalies allow a comparison of Geosat and Seasat with the FDM. The median difference between the anomalies according to Geosat and the anomalies according to the FDM amounts to 0.12±0.21 m (see Fig. S6). Considering that this difference is very sensitive to extrapolating the respective long-term trends, this is a remarkable agreement. With a median of 0.26±0.32 m, the difference between anomalies from Seasat and from the FDM is larger, but this comparison is also more vulnerable to potential errors due to the extrapolation. As the FDM starts in

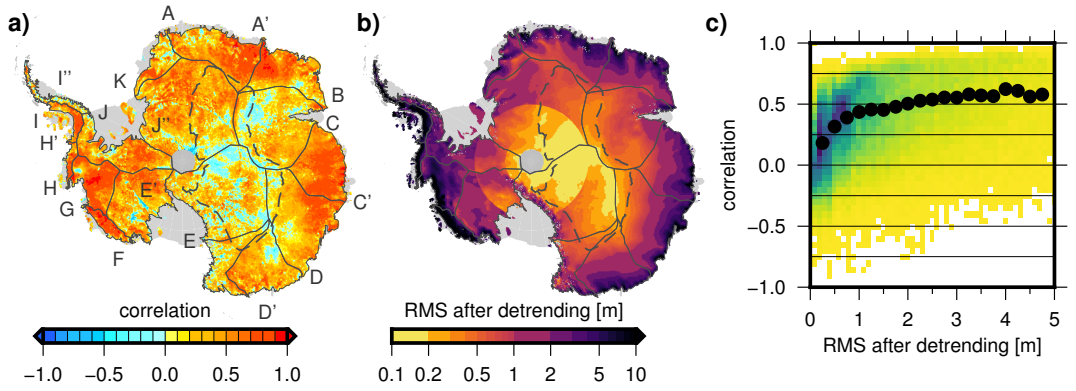

Figure 8. **a)** Correlation coefficient between the SEC anomalies of the altimetry grids and the FDM over 1992-2016 after detrending. **b)** RMS of the detrended anomalies of the 1992-2016 altimetry time series. **c)** Correlation coefficient plotted against the RMS. The point density is color coded from yellow to blue. The black dots show the binned mean values.

1979 while Seasat operated in 1978, we compare the Seasat data with the FDM anomalies from the respective months of 1979, which might impose additional differences. Finally, the FDM model has its own inherent errors and uncertainties. Therefore, only part of the differences originates from errors in the altimetry results.

5 Results

5.1 Surface elevation changes

Some examples for elevation change time series in the resulting multi-mission SEC grids are shown in Fig. 9 (coordinates in Tab. S2). For Pine Island Glacier (PIG, Fig. 9a), we observe a continuous thinning over the whole observational period since 1992 (Seasat and Geosat measurements do not cover this region). Close to the front (point D) the surface elevation decreased by -45.8±7.8 m since 1992, which means an average SEC rate of -1.80±0.31 m/yr. The time series reveals that this thinning was not constant over time, but accelerated near the grounding line (point D and C at a distance of 40 km~~spatial resolution from the approach described above. Five examples given in Fig.6a demonstrate the spatial coverage and~~) around 2006. Also the points at greater distances from the grounding line (B at 80 km, A at 130 km) show an acceleration around 2006. After 2010, the thinning rates at near front decelerate again. For the period 2013-2017, the rate of -1.3±0.8 m/yr is very close to the rate preceding the acceleration. In contrast, further inland the thinning did not decelerate so far and is still at a level of about -1.2 m/yr. Hence, for the most recent period (2013-2017) the elevation at all points along the 130 km of the main flow line is decreasing at very similar rates. A similar acceleration near the grounding line, followed by slowdown, is observed by (Konrad et al., 2016). The onset of this acceleration coincides with the detaching of the ice shelf from a pinning point (Rignot et al., 2014). After that speedup terminated around 2009, the grounding line position was relatively stable (Joughin et al., 2016), which agrees with the elevation changes in our observations.

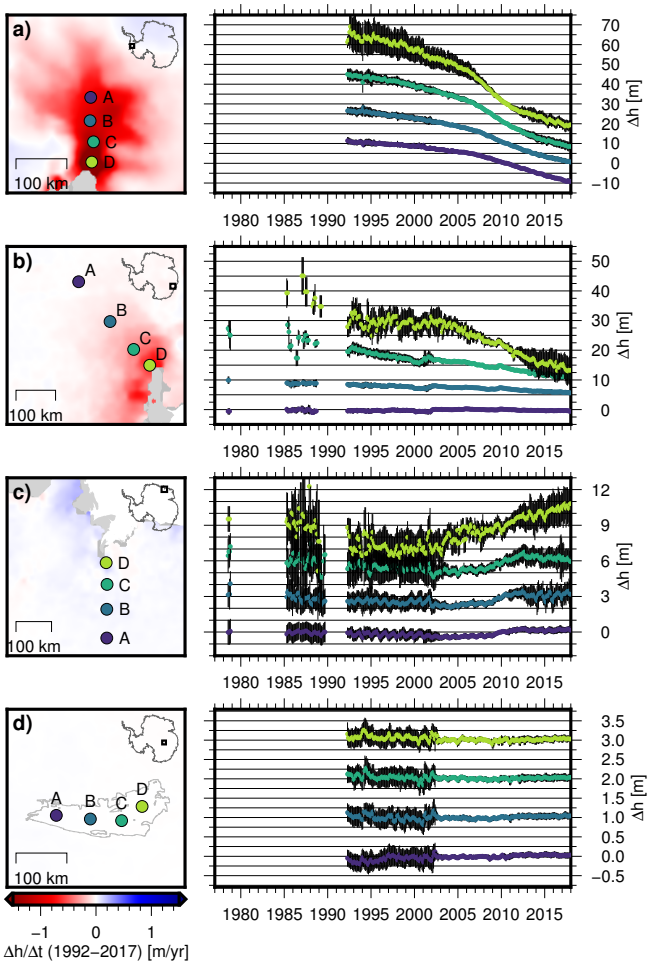

Figure 9. Multi-mission SEC time series in 4 selected regions (**a)** Pine Island Glacier, **b)** Totten Glacier, **c)** Shirase Glacier in Dronning Maud Land and **d)** Lake Vostok). The time series of point B, C and D are shifted along Δh for better visibility. The maps on the left show the elevation change between 1992 and 2017 as in Fig. 10b.

Also for Totten Glacier in East Antarctica (Fig. 9b), we observe a clear negative SEC. This has been previously reported by several authors (e.g. Pritchard et al., 2009; Flament and Rémy, 2012; Zwally et al., 2015) but our data provide an unprecedented time span and resolution. At the very grounding line (point D), Totten Glacier thinned by 31.8±7.7 m between 1987 and 2017, which results in an average SEC rate of -1.0±0.2 m/yr. Seasat could not provide successful observations at the very grounding line but the time series for point C (around 60 km inland) with a rate of -0.38±0.10 m/yr between 1978 and 2017 and for point B (150 km) with a rate of -0.11±0.04 m/yr, respectively, indicate that this thinning already preceded before the epoch of Geosat. At point A in a distance of 280 km, we find no significant elevation change (0.01±0.03 m/yr for 1978-2017). The temporal resolution of these data allows us to analyze the change over time. While we see a significant thinning at the grounding line between 1987 and 1994 of 16.6±9.8 m, the elevation stabilized between 1994 and 2004 to within ±1.5 m. After 2004, the

grounding line thinned again by 15.4±5.5 m until 2017. Li et al. (2016) observe a similar variation in ice velocity measurements between 1989 and 2015. Combining their ice discharge estimates with surface mass balance, they obtain a relatively large mass imbalance for Totten Glacier in 1989, decreasing in the following years to a state close to equilibrium around 2000. After 2000, they observe an acceleration of ice flow, again consistent with our thinning rates. The authors attribute this high variability to variations in ocean temperature. In another study, Li et al. (2015) observe a grounding line retreat at Totten Glacier of 1 to 3 km between 1996 and 2013 using SAR Interferometry. They conclude that this indicates a thinning by 12 m, which is again consistent with our results over this period (12.0±8.8 m).

At Shirase Glacier in Dronning Maud Land (DML, Fig. 9c), we observe a relatively stable surface with a slightly negative change rate between 1978 and the early 2000s. In this region, two significantly positive accumulation anomalies occurred in 2009 and 2011 (Boening et al., 2012; Lenaerts et al., 2013). The increase in surface elevation associated to these event is visible in our time series. At point C, the elevation changed by 1.0±1.5 m between 2008 and 2012. Even at point A, more than 200 km inland and at an altitude of 2500 m, the elevation increased by 0.55±0.50 m during this time. At point D, a similar jump is observed in 2003, which corresponds to another SMB anomaly (cf. Fig. 2a in Lenaerts et al., 2013).

In contrast to the regions discussed so far, the ~~ability to resolve the temporal evolution. The time series along the profile from Totten Glacier to Lake Vostok (Fig.6b) shows the consistency of the data, including the two early missions. Especially in the coastal areas where the signals are large, the early missions can provide important information to extend the time interval by additional 15 years.~~ elevation change on the plateau of East Antarctica is very small. The time series for four different points at Lake Vostok (Fig. 9d) show rates which are very close to zero (point A: 5±9 mm/yr, B: -1±10 mm/yr, C: -3±9 mm/yr, D: -1±10 mm/yr between 1992 and 2017). The larger variations in the ERS time series is a result of the lower resolution of the waveform in the ice mode of the ERS satellites. These rates contradict the findings of Zwally et al. (2015). They report a surface elevation increase of 20 mm/yr over Lake Vostok, which would result in an increase of elevation of 0.5 m over the period 1992-2017. Our results are confirmed by ground based static GNSS observations (Richter et al., 2008, 0.3±4.9 mm/yr), kinematic GNSS profiles measured around Vostok Station using snow mobiles (Richter et al., 2014, 1±5 mm/yr) and by GNSS profiles using traverse vehicles over the entire Lake Vostok region (Schröder et al., 2017, -1±5 mm/yr).

~~Surface elevation change rates fitted to the combined SEC time series over different time intervals are given in Fig.10.For the interval~~ The full pattern of surface elevation changes is shown in Fig. 10. These change rates are obtained by calculating elevation differences between the respective years, divided by the time difference. To reduce remaining noise, we use yearly averages (January-December). If one of the years does not cover the full annual cycle, we calculate the average only from the months covered in both years (July-October for 1978-2017~~these rates show which processes persist over four decades. Due to the orbit inclination of the early missions, these results are mainly limited to coastal areas in East Antarctica but also some flat regions along the Antarctic Peninsula are covered by observations of the early missions. A spatially more comprehensive picture is given in Fig. 10b~~, ~~covering the~~ April-December for 1992-2017). We calculate the SEC rate from epoch differences instead of fitting a rate to all epochs because the first observations at specific latitudes start in different years, the observations have different precisions and the large gap between 1978 and 1985 is not covered by observations at all. These three points

~~Multi-mission surface elevation change rates from the combined SEC time series over different time intervals. The solid lines mark the drainage basin outlines, the dashed line shows the outline of the low precipitation zone. **a)** Trends for the area covered by observations since 1978. **b)** Trends since 1992 for the area covered by the ERS missions and Envisat. **c-e)** consecutive time intervals show coherent patterns in dynamic regions but also large variations due to interannual variability.~~

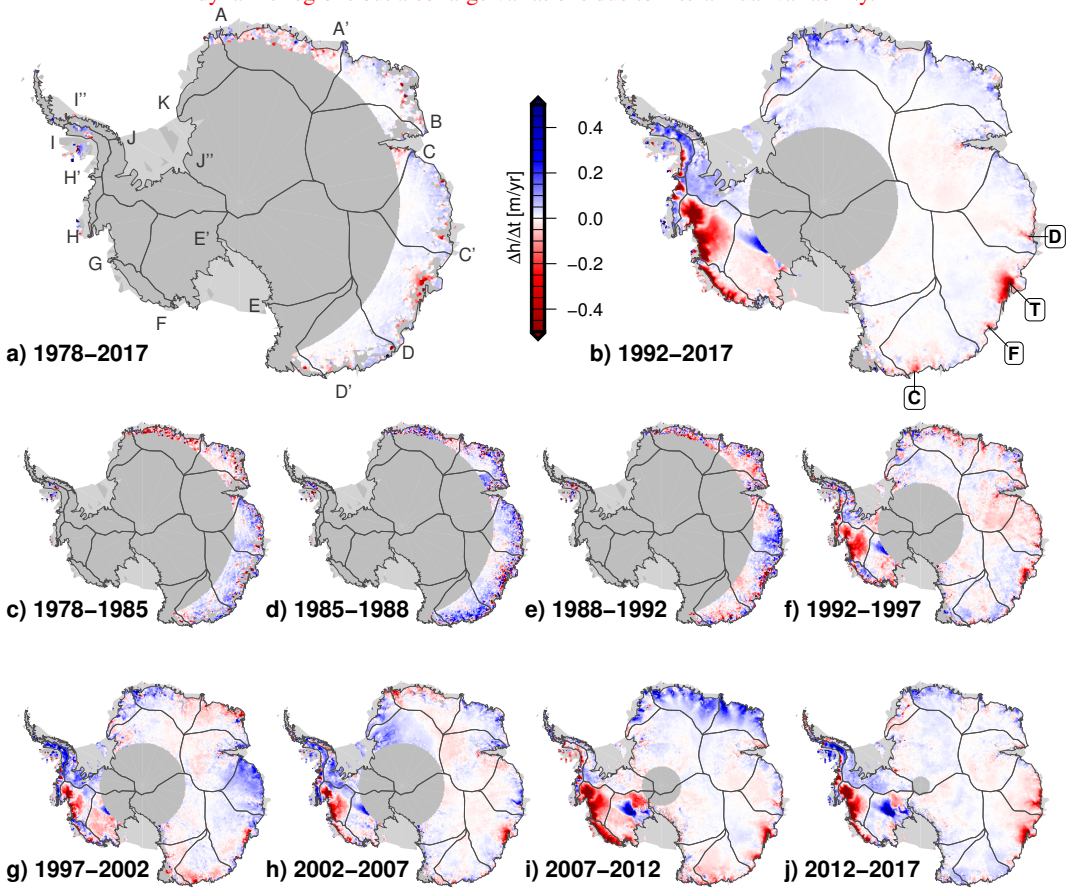

Figure 10. Multi-mission surface elevation change from the combined SEC time series over different time intervals. **a** and **b)** The long-term surface elevation change between 1978 and 2017 and 1992 and 2017 for the respectively covered area. **c-j)** Elevation change over consecutive time intervals reveal the interannual variability. Thin lines mark the drainage basin outlines, denoted in **a**. Bold letters in boxes in **b** denote glaciers, mentioned in the text.

would lead to a bias towards the later epochs in a fit, which would not be representative for the true average elevation change over the full interval.

The long-term elevation changes over 25 years (Fig. 10b) show the well known thinning in the Amundsen Sea Embayment and at Totten Glacier, as well as the thickening of Kamb Ice Stream (cf. e.g. Wingham et al., 2006b; Flament and Rémy, 2012; Helm et al., 2 . In contrast, 60% of East Antarctica north of 81.5°S shows surface elevation changes of less than ±1 cm/yr. However, several coastal regions of the EAIS show significant elevation changes, too. Totten Glacier (T in Fig. 10b) is thinning at an average

rate of 72±18 cm/yr at the grounding line (cf. Fig. 9b). Several smaller glaciers in Wilkes Land also a persistent thinning. We observe SEC rates of -26±10 cm/yr at Denman Glacier (D), -41±19 cm/yr at Frost Glacier (F) and -33±12 cm/yr near Cook Ice Shelf. Rignot (2006) showed that the flow velocity of these glaciers, which are grounded well below sea level, was above the balance velocity for many years. In contrast, the western sector of the EAIS (Coats Land, DML and Enderby Land, basins J"-B) shows thickening over the last 25 ~~years since the launch of ERS-1. Similar rates calculated over sub-intervals of~~ years at rates of up to a decimeter per year.

Comparing the long-term elevation changes over 40 years (Fig. 10a) with those over 25 years shows the limitations of the early observations, but also the additional information they provide. There were only relatively few successful observations at the very margins but e.g. for Totten or Denman Glacier, they show similar rates at a distance of about 100 km from the grounding line. In DML and Enderby Land (basins A-B in Fig. 10a), the 40 yr interval shows less positive rates, compared to 1992-2017. Until 2002, a large part of this region even experienced significant thinning (see time series in Fig. 9c and the maps for the ~~full timerange, namely 07/1978-12/1992, 04/1992-12/2010 and 01/2010-12/2017, are displayed in the panels c-e. The interval 1978-1992 shows that coherent results can also be obtained from the first 15 years by the early missions in these regions. From panels d and e, compared to 1992-2017, we see that the large persistent change rates, which are mainly related to ice dynamics, can also be observed over shorter time intervals. However we also see significant differences between the two intervals, leading to the conclusion that interannual variations or changing ice dynamics may have a strong influence on these time intervals. Hence, to study the temporal variability of the observed elevations, in the following we analyzed the full time series over different spatial and temporal scales.~~ sub-intervals in Fig. 10c-g). After that time, especially over the period 2007-2012 (Fig. 10i), this region shows a huge increase in elevation, which relates mainly to the accumulation events in 2009 and 2011. The sub-intervals in Fig. 10c-j demonstrate the effect of interannual snowfall variability on the elevation change rates over shorter time intervals. They show similar variations also in other regions, pointing out that accumulation events have a strong influence on interannual elevation changes over all parts of Antarctica (Horwath et al., 2012; Mémin et al., 2015).

~~Volume change of the Antarctic Ice Sheet north of 81.5°S (**a**) and the three subregions (**b** EAIS, **c** WAIS and **d** APIS) from our combined altimetric time series (blue). The respective time series of mass change from GRACE (red) and precipitation anomaly (pink) refer to the scale at the right. The gray color in the background displays the fraction of the area covered by observations (up to the top means 100%). Subfigure **e** shows the mean surface elevation change in the low precipitation zone north of 81.5°S. The scale on the right here refers to the water equivalent precipitation anomaly (pink) and was scaled by factor 3 to resemble an elevation change due to fresh snow.~~

5.2 Ice sheet mass time series

~~Elevation difference between the yearly mean SEC (July to June of next year) of consecutive years. Marked in yellow are differences spanning more than one year due to altimetry data gaps.~~

~~At scales of subregions of the Antarctic Ice Sheet or drainage basins we calculated cumulative volume time series, shown in Fig.11 and 13. Therefore, we multiplied the elevation time series by the corresponding grid cell area and summed them up over the respective region. We used amodified version of the drainage basin definitions by Rignot et al. (2011). This set was~~

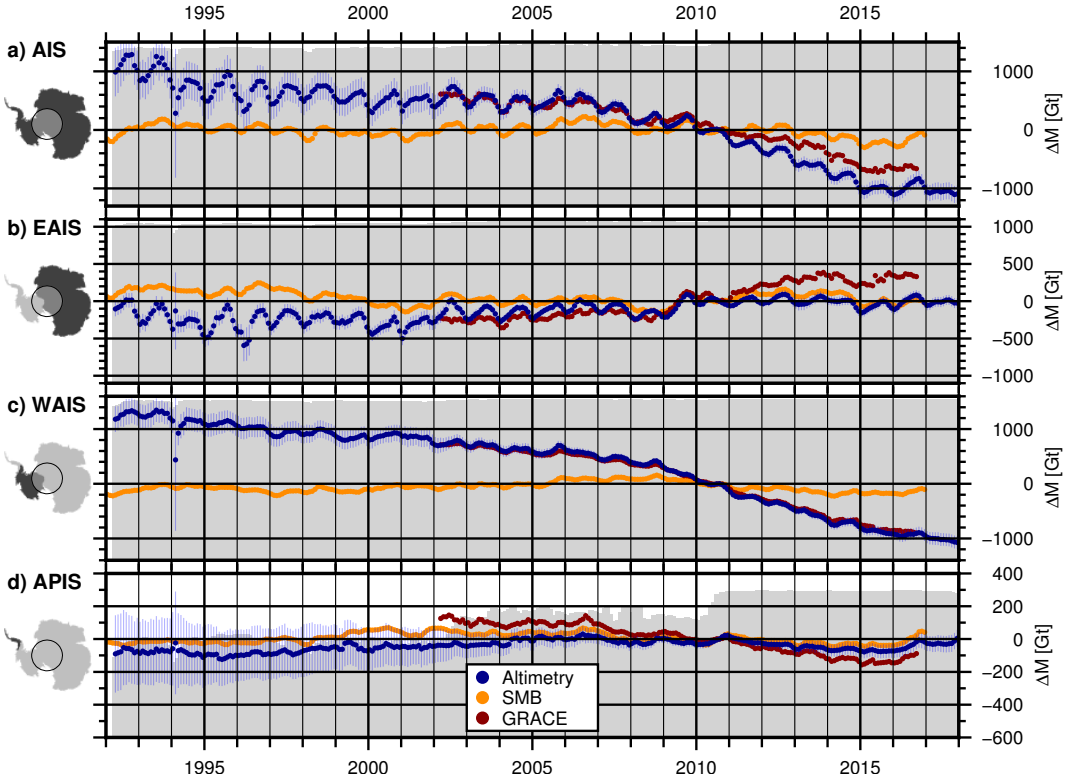

Figure 11. Mass change of the Antarctic Ice Sheet north of 81.5°S (**a**) and the three subregions (**b** EAIS, **c** WAIS and **d** APIS) from our combined altimetric time series (blue), GRACE (red) and SMB (orange). The error bars show the uncertainty estimate σ_Σ of the altimetry data according to Sect. F.2. The gray color in the background displays the fraction of the area covered by altimetry (up to the top means 100%).

~~modified for an update of the ice sheet mass balance inter-comparison exercise (IMBIE, Shepherd et al., 2012) and is depicted in Fig.10a. To correct for elevation changes due to GIA, all time series were corrected using the model~~ In order to determine the effect of the SEC on global sea level, they are converted to ice mass changes. In a first step, all time series are corrected for glacial isostatic adjustment (GIA) using the IJ05_R2 ~~(Ivins et al., 2013). This GIA-model~~ model (Ivins et al., 2013). This GIA model predicts an uplift of 5 $\mathrm{mm/yr}$ near the Antarctic Peninsula and rates between -0.5 and +2 $\mathrm{mm/yr}$ in East Antarctica. ~~The average GIA over the area of the entire ice sheet is 0.6~~Furthermore we applied a scaling factor $\alpha = 1.0205$ to account for elastic solid earth rebound effects (Groh et al., 2012). We multiply the resulting ice sheet thickness changes by each cell's area and apply a density according to a firn/ice mask (McMillan et al., 2014, 2016), depicted in Fig. S8, to obtain a mass change. In regions where ice dynamic processes are assumed to be dominating (e.g. in Amundsen Sea Embayment, Kamb Ice Stream or Totten Glacier), we use a density of 917 ~~which translates to a volume changerate of 7.4~~$\mathrm{kg/m^3}$. Elsewhere, we apply the density of near-surface firn, obtained from firn modeling using atmospheric forcing (Ligtenberg et al., 2011). We have chosen this straightforward and robust method here, instead of using modeled temporal variations of the firn layer

~~Volume change of subregions north of 72°S for several East Antarctic drainage basins from our combined altimetric time series (blue). The respective time series of mass change from GRACE (red) and precipitation anomaly (pink) refer to the scale at the right. The gray color in the background displays the fraction of the area covered by observations.~~

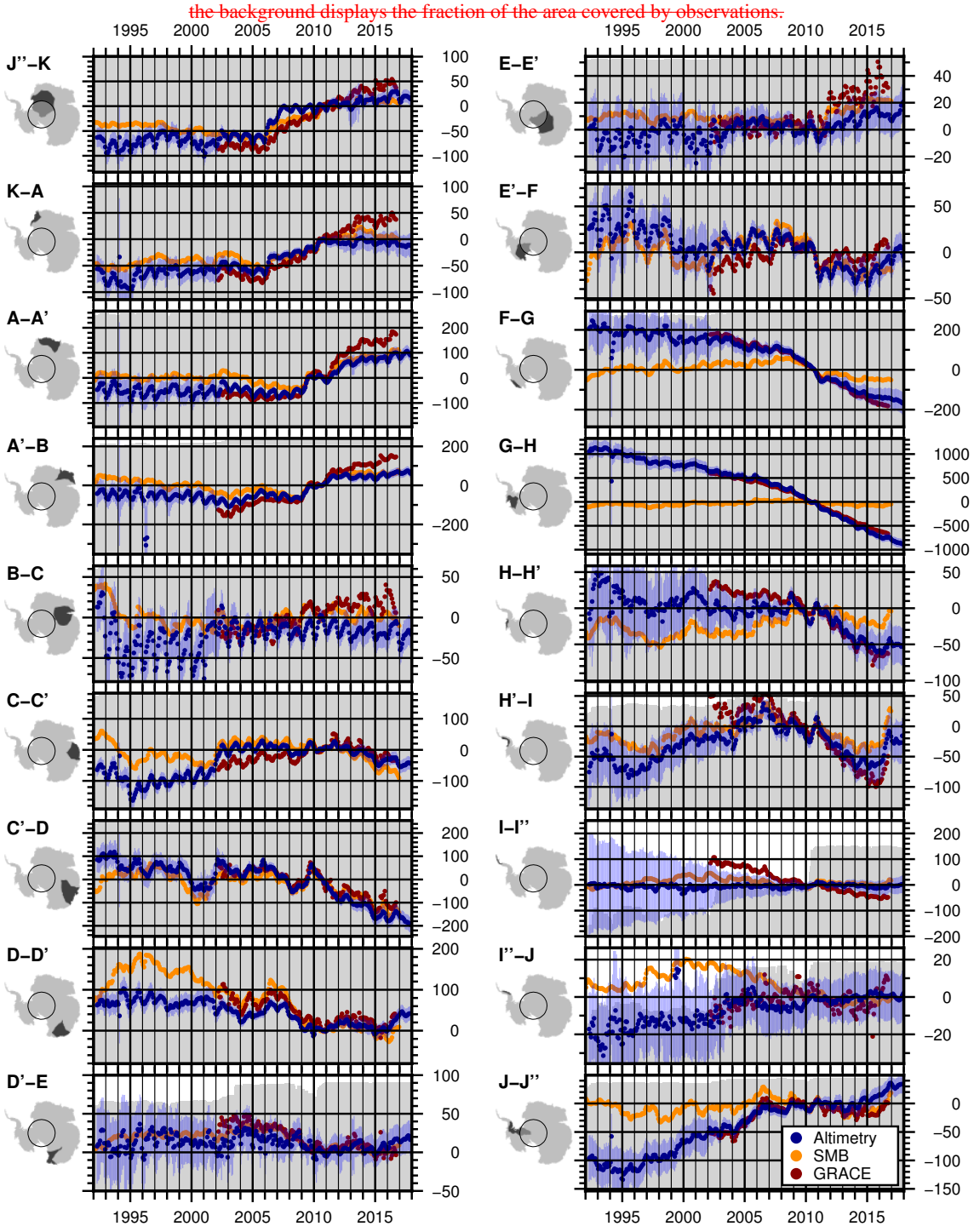

Figure 12. Mass change ($\Delta M[Gt]$) of the individual drainage basins north of 81.5°S from our combined altimetric time series (blue), GRACE (red) and SMB (orange). The error bars show the uncertainty estimate σ_Σ of the altimetry data according to Sect. F.2. The gray color in the background displays the fraction of the area covered by altimetry (up to the top means 100%).

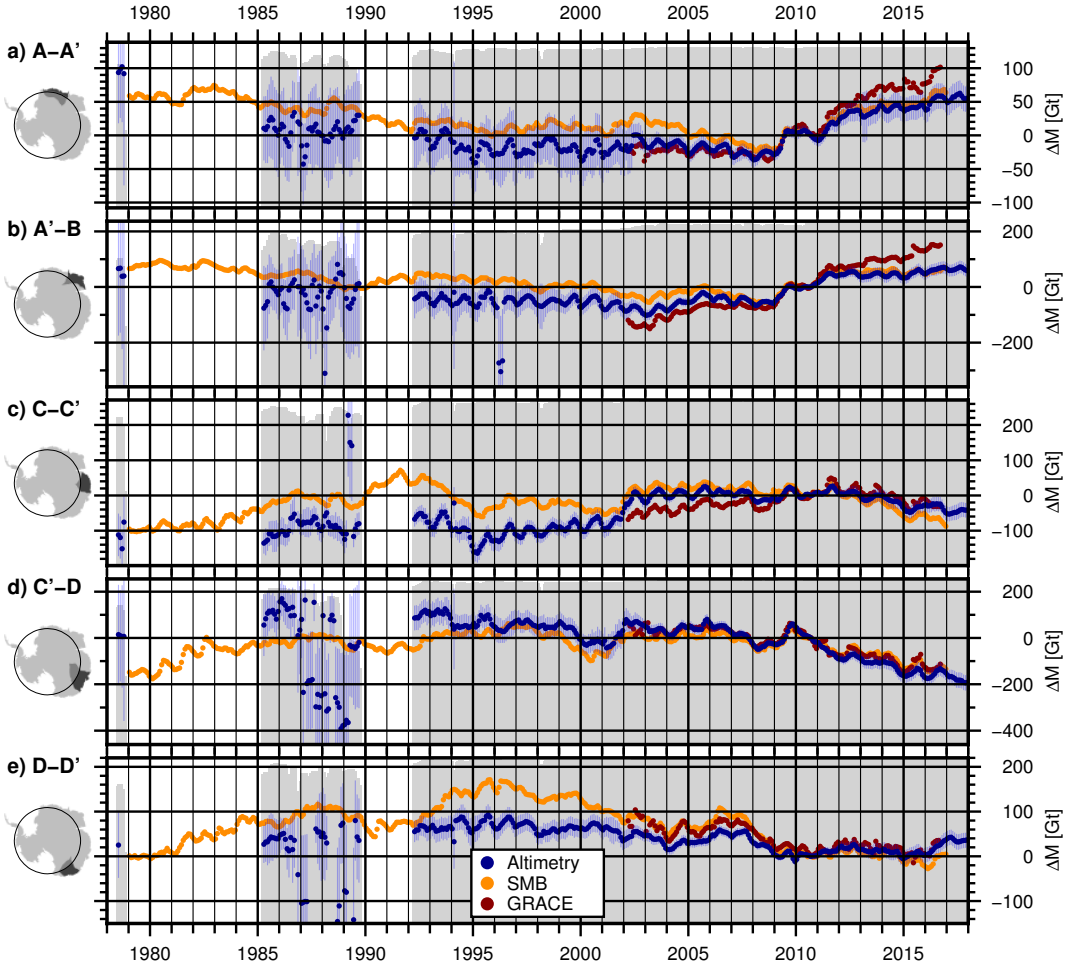

Figure 13. Mass change of subregions north of 72°S for several East Antarctic drainage basins from our combined altimetric time series (blue), GRACE (red) and SMB (orange). The error bars show the uncertainty estimate σ_Σ of the altimetry data according to Sect. F.2. The gray color in the background displays the fraction of the area covered by altimetry (up to the top means 100%).

(as e.g. Zwally et al., 2015; Kallenberg et al., 2017) in the volume-to mass conversion. This allows us to compare the time series from altimetry with time series from SMB modeling.

Cumulated mass anomalies over larger regions such as drainage basins or even the total AIS are obtained by summing up the results accordingly. Therefore, we used the basin definitions by Rignot et al. (2011) (updated for Shepherd et al. (2018) , see Figs. ~~. Cells containing no valid data after~~ 10a and 14b). Cells containing no valid data after the gridding (as e.g. where not enough observations were available, in the polar gap or where rocks are predominant) are not considered here. Uncertainty estimates were obtained by propagating the respective uncertainties of the SEC, the ~~gridding, e.g. in~~ GIA and the ~~polar gap or where rocks are predominant, are not considered in these sums. The fraction of valid cells at each epoch is shown in the background of the plots. To support the interpretation of trends, peaks and jumps in the time series, we~~

compare the respective time series of cumulative precipitation anomalies from ECMWF ERA-Interim (Dee et al., 2011) and GIA-corrected GRACE mass balances (Groh and Horwath, 2016) to our data. A direct comparison would impose the need to convert our volume changes to mass. This conversion, however, is subject of controversial discussions whether a density mask (e.g. Sørensen et al., 2011; McMillan et al., 2014) is appropriate or if a firn densification model (e.g. Zwally et al., 2015; Kallenberg et al., is able to correctly model the interannual to decadal variations, especially in East Antarctica. As this is beyond the scope of this paper, all mass time series data are plotted at a scale of 1/3 of the volume scale. Hence, for a mass variation of fresh snow the curves would be directly comparable while for a mass loss or gain at a higher density, the mass curves vary stronger than the volume curvefirn density to the basin sums for each month (see Sect. F.2 for details). We also include an estimate for the effect of unobserved cells in the error budget.

Figures 11a-d show the time series summed up over the entire Antarctic Ice Sheet time series for the entire AIS north of 81.5°S (i.e. covered by radar satellite altimetry since 1992), and the subregions of East Antarctica, West Antarctica and the Antarctic Peninsula. In the supplementary material, Fig. S6 and S7 show similar time series for each individual drainage basin. Furthermore, we used the ERA-Interim data to define the low precipitation zone (LPZ) similar to Gunter et al. (2014) where the average annual precipitation is less than 20 water equivalent. This area is of particular interest as it has been used by Gunter et al. (2014) to determine ICESat inter-campaign biases while Zwally et al. (2015) argue that this zone might be prone to dynamic thickening and thus the calibration might be offset. To support the interpretation in the LPZ, Fig.11e shows the mean SEC instead of the volume time series for this region. The full time interval of radar altimetry measurements of the Antarctic Ice Sheet is shown in Fig.13respective subregions EAIS, WAIS and the APIS. Similar time series for the single drainage basins over 1992-2017 are shown in Fig.The time series here are generated for subregions of basins which have a reasonable extent beyond 12. The full four decade time interval for the coastal areas of the EAIS is shown in Fig. 13. These time series use the data north of 72°S and thus are observed for the first time in only and, hence, provide a nearly consistent observational coverage since 1978.

The spatial pattern of the elevation changes from year to year are shown in Fig. **??**. Yearly averages are calculated from July until June of the next year and subtracted from each other. For 1978, the average is calculated from July to October only, the mission lifetime of Seasat. For the last period , denoted as "17", the average spans from July to December. The time intervals marked in yellow refer to differences that span more than one year. A similar plot for the precipitation anomaly data can be found in the supplementary material (Fig. S8).

To summarize the results we fitted trends to the volume change time series over Antarctica and several subregions which are listed in Tab. **??**. It should be noted that , due to the different orbit inclinations of the missions, only the respectively covered regionscan be used to calculate trends. The omissions of the ERSTo support the interpretation and evaluate the temporal evolution, we compared the respective time series to GIA-corrected cumulated mass anomalies from satellite gravimetry (GRACE, Groh and Horwath, 2016). To reduce the effect of noise in the GRACE monthly solutions and to make the data more comparable to our altimetry results, we applied a three-month moving average to the GRACE time series. We also compare our data to time series of cumulated surface mass balance anomalies from RACMO2.3p2 (SMB, van Wessem et al., 2018). Similar to the firn model, the SMB contains seasonal and interannual variations due to surface processes. However, it assumes an

equilibrium over the modeled period and, hence, does not include long-term changes. The different time series show the good agreement of the techniques in resolving interannual variations. For example for the basin of Totten Glacier (C'-D in Fig. 12), all techniques observe a negative mass anomaly in early 2008, followed by a significant mass gain in 2009. Between 03/~~Envisat polar gap can be assessed, at least for the period 2010-2017, by comparing the volume trends that respectively include and exclude the area south of 81.5°S. The difference (-151±14~~2008 and 10/2009, we obtain a mass difference of 116.6±27.0 ~~versus -170±11~~Gt from altimetry, 109.4 ~~)is as low as 19~~Gt from SMB and 113.4 ~~. The error measure given with the rates here is~~ Gt from GRACE. The high agreement with the SMB indicates that this mass gain is caused by snow accumulation. In most of the basins, we observe similar high agreement in the short-term variations. A good example for the different components of the total mass change signal is the Getz and Abbot region (F-G). While all techniques observe a significant mass loss between 2009 and 2011, the ~~standard deviation from the linear fit. In the stochastic model, also a covariance between consecutive epochs has been considered but systematic sources of error could not be accounted for, hence our error estimate tends to be too optimistic.~~ SMB does not contain a long term trend, as observed by altimetry and GRACE. In some regions, however, there are also significant discrepancies between the different data sets. The poor sampling of the northernmost APIS (I-I") by altimetry is a good example for the limitations of this technique. In George V Land (D-D'), the agreement during the GRACE period is reasonable, while the mass gain, indicated by the SMB in the early 1990s is not revealed by the altimetry time series.

~~Comparing the rates over different time periods reveals that fitting a linear trend is highly dependent on the time intervalused.For the whole ice sheet north of 81.5°S we obtain an average volume rate of -34±5~~Over the last 25 years our data indicate a clearly negative mass balance of -2068±377 ~~for 1992-2017. Separating the time series at 2010 when several glaciers started to accelerate, we obtain a slightly positive rate (27±5~~Gt for the AIS (Fig. ~~) for 1992-2010 but a dramatically larger volume loss of -170±11~~11a). This is mainly a result of the mass loss in the WAIS over the last decade. In contrast, the EAIS has been very stable over our observational record (120±121 ~~for 2010-2017. This again points out that linear rates are only comparable when they refer to the same time interval~~Gt between 1992 and 2017). The time series of the APIS contains large uncertainties due to many unobserved cells. Mass change rates for selected regions, obtained from the differences over a specific time interval, and their respective uncertainties are given in Tab. 2. We calculated separate trends for the area north of 72°S, which is covered by all satellites, north of 81.5°S which is covered since ERS-1 and for the total area, which is (except the 500 km diameter polar gap) covered since CryoSat-2. The observed area shows that 96.4% of the cells, classified as ice sheet north of 81.5°S, are successfully covered by observations of ERS-1. Cells without successful observation occur mostly at the APIS, where only 61% is covered with data.

~~Map (**a**) and histogram (**b**) of elevation differences observed at crossover locations of GNSS profiles minus the elevation difference obtained from the altimetric results for the respective times.~~

~~To validate our results, we used a set of 19 kinematic GNSS profiles (Schröder et al., 2017). They have been observed between 2001 and 2015 and most of the profiles cover more than 1000~~From the overall mass loss of -2068±377 ~~. The accuracy RMS_{KIN} of the surface elevation profiles was assessed by a crossover comparison between independent profiles of the same season. It is in the range of 4 to 9 . One profile (K08C) has not been used as the poorly determined antenna height offset might impose larger errors. In Schröder et al. (2017) we used these profiles to validate the absolute altimetric elevation~~

Table 2. ~~Volume~~ Mass change ~~rate~~ rates for ~~Antarctica (ANT),~~ different regions of the ~~East and West~~ Antarctic Ice Sheet ~~(EAIS~~ and ~~WAIS)~~ ~~and the Antarctic Peninsula (APIS)~~different time intervals. The ~~size~~ sizes of the total and observed area ~~refers~~ refer to ~~observations from: Seasat for latitudes north of 72°S, ERS-1/2 for latitudes north of 81.5°S~~ all cells classified as ice sheet in the respective region (and~~CryoSat-2 for regions without a southern limit. The very sparse observations of Seasat and Geosat on~~ , if stated, limited by the ~~Antarctic Peninsula do not allow to calculate a reliable long-term trend~~given latitude).

region	area [10^3km^2]		dM/dt [Gt/yr]			
	total	observed	1978-2017	1992-2017	1978-1992	1992-2010
~~ANT~~ AIS	11892	~~11658~~ 11630	-	-	-	~~-151.3~~ -
~~ANT (<81.5°)~~ EAIS	~~9391~~ 9620	~~9194~~ 9413	-	~~-33.84.8~~ -	~~26.94.9~~ -	~~-169.8~~ -
~~ANT (<72°)~~ WAIS	~~2913~~ 2038	~~2259~~ 2008	~~12.71.4~~ -	~~19.01.8~~ -	~~31.32.6~~ -	~~-27.7~~ -
~~WAIS~~ APIS	~~2038~~ 232	~~2011~~ 208	-	-	-	~~-145.2~~ -
~~WAIS~~ heightAIS (<81.5°S)	~~1394~~ 9391	~~1372~~ 9053	-	~~-94.3~~ -84.7±~~3.0~~ 15.5	~~-51.7~~ -	-58.6±~~2.2~~ 20.3
~~APIS~~ EAIS (<81.5°S)	~~232~~ 7764	~~180~~ 7555	-	~~0.8~~4.9±~~0.7~~ 5.0	~~12.1~~ -	8.0±~~0.6~~ 6.2
~~EAIS~~ WAIS (<81.5°S)	~~9620~~ 1394	~~9435~~ 1358	-	~~-~~ -91.7±10.3	-	~~2.6~~-69.4±~~7.1~~ 13.1
~~EAIS~~ APIS (<81.5°S)	~~7764~~ 232	~~7642~~ 142	-	~~54.1~~2.1±~~2.5~~ 8.9	~~61.7~~ -	2.8±~~3.8~~ 12.3
EAIS (<72°S)	2779	~~2247~~ 2274	~~12.0~~1.5±~~1.4~~ 5.8	~~17.4~~ 3.4±~~1.7~~ 4.0	~~26.2~~12.1±~~2.5~~ 17.4	~~-20.7~~0.0±~~3.9~~ 4.9

For the APIS (<72°S), the very sparse observations of Seasat and Geosat did not allow calculate a reliable trend.

~~measurements. Here, we only work with elevation differences w.r.t. a reference epoch. As we want to analyze the temporal variability, we compare elevation changes over the same time observed by both techniques . For each crossover difference between kinematic profiles from different years we compare the differences of the respective altimetric SEC epochs in this location ($\delta\Delta h = \Delta h_{KIN} - \Delta h_{ALT}$). Figure 7 shows the results of this validation. We obtain an overall agreement of 6±16~~Gt for the AIS (<81.5°S over 1992-2017) we obtain an average long-term rate of -84.7±15.5 ~~or an RMS of 17.7~~Gt/yr. This rate agrees within error bars but is considerably smaller than the results of Shepherd et al. (2018) of -109±56 ~~. As both techniques should observe the same elevation change,~~ Gt/yr. However, the ~~difference $\delta\Delta h$ can be interpreted as an error measure. It can be expressed as~~

$$\delta\Delta h^2 = 2 \cdot RMS_{ALT}{}^2 + 2 \cdot RMS_{KIN}{}^2$$

~~as two kinematic profiles (with the respective RMS_{KIN}) and two altimetric epochs (with RMS_{ALT}) contribute to this difference. Using the a priori RMS_{KIN} (4-9) and resolving for RMS_{ALT} yields the empirical RMS of the altimetric SEC data which lies in~~ extended material in Shepherd et al. (2018) shows that there are still some discrepancies between the different techniques to determine the AIS mass balance. For the ~~range between 8 and 12~~time interval 2003-2010 (Extended Data Table 4 in Shepherd the Input-Output method obtains a rate of -201±82 ~~. A comparison with the satellite altimetry measurement precision (Tab. **??**) shows that this corresponds to what we expect from the underlying measurements. The majority of the profiles was observed~~

between 2007 and 2015. Hence, the differences also include different missions and observation techniques. So, we can conclude that no significant additional uncertainty has been added due to the combination. Small positive or negative biases in some regions of the map could be attributed to remaining antenna height offset errors in one of the GNSS profiles, but might also originate from remaining penetration effects of the radar signals. The very high agreement between the two datasets shows that our processing successfully eliminated the biases between the different satellite altimetry missions and thus provides reliable results Gt/yr for the AIS, while the mass balance rates, aggregated from satellite gravimetry (-76±20 Gt/yr) and from altimetry (-43±21 Gt/yr) agree much better with our result for the AIS (<81.5°S) between 2003 and 2010 of -64.7±24.9 Gt/yr. Nevertheless, only altimetric SEC within the

6 Discussion

6.1 Multi-mission SEC time series

The single-mission time series, obtained in Sect. 3.2, contain satellite-specific calibration biases as well as offsets due to the specific sampling characteristics of different sensor types. In order to form a consistent SEC time series, these biases needed to be determined and corrected. A comparison with in situ data showed that there are no significant offsets between elevation changes from our multi-mission altimetry data and the validation datasets. This comparison, however, could only validate our data in the interval 2001-2015 can be validated in this way. For the earlier missions, no spatially extensive high precision in situ data are available to us. 2001-2016. A quality control for the whole time span was performed by a comparison with a firn model. The correlation of the detrended data sets shows that especially for regions where the interannual variation is large (compared to the measurement noise of the altimeters) both time series agree very well. This comparison even provided independent estimates for the error of the early missions. The average differences between the detrended time series of the FDM and the SEC show that the observations of Geosat and even of Seasat agree with the model results within a few decimeters. For SECs of up to several meters w.r.t 2010 (see Fig. 6), this means that also the older data can be used to calculate elevation change rates with an accuracy better than a centimeter per year (see Fig. S7a). Unfortunately, in coastal DML west of the ice divide A', the data of Seasat and Geosat are very noisy. This due to the mountain ranges just north of 72°S, which lead to many losses of lock of the measurements all the way across this part of the ice sheet. The same applies to the measurements at the APIS.

7 Interpretation and Discussion

6.1 Surface elevation changes

The linear elevation change rates in Fig. mean rates of elevation change in Fig. 10 show the regions which experience a significant thinning (Amundsen Sea Embayment, Totten Glacier) or thickening (Kamb Ice Stream) which was already shown by a range of previous publications (e.g. Wingham et al., 2006b; Flament and Rémy, 2012; Helm et al., 2014). In contrast to those studies our rates are calculated from the combined time series and hence, cover a much longer time interval of 40 yearsfor the

coastal regions of East Antarctica(Fig. 10a) and reported by previous publications (e.g. Wingham et al., 2006b; Flament and Rémy, 2012; F
. By combining all the single missions consistently we analyze long-term changes over the full time period covered. For 79% of the area of the AIS, this means a time span of 25 years. For 25years also for large parts of the interior of the ice sheet (Fig.10b). In both of these %, mainly the coastal regions of East Antarctica, even 40 years are covered. We assume that these long-term trends we see elevation gains of several along the Antarctic Peninsula and in most of trends are significantly less affected by short-term variations in snowfall than a trend from a single mission.

The benefits of a seamless combination of the time series are demonstrated in Fig. 10. The time intervals for the elevation changes are independent of the coastal regions of East Antarctica between 45°W and 110°E. In Wilkes Land (C'-D') we see persistent rates of volume losses not only at Totten Glacier but also on some smaller glaciers as Frost, Mertz, Ninnis and Cook Glacier. Rignot (2006) observed previously that these glaciers, which are grounded below sea level, are thinning and losing mass. Our 25 year interval furthermore reveals the stability of the interior of the East Antarctic Ice Sheet. For 54% of the observed area of East Antarctica (north of 81.5°S), we find that the surface elevation changes are less than ±1observational period of a single mission. This is necessary to analyze processes which occurred close to the transition between different missions. A good example of the advantage of such long time series are the elevation changes caused by the accumulation events in DML. Figure .

The different sub-intervals in Fig.10c-e show that the spatial pattern of elevation changes in East Antarctica is not constant over time. During 1978-1992 the East Antarctic sector west of the Amery Ice Shelf (A-B) was losing volume while in the eastern sector (C-D') the rates were mainly positive. For the interval 1992-2010 we see positive rates in Coats Land and western Dronning Maud Land (J"-A') 9c clearly shows the changes in elevation, caused by the strong snowfall events in 2009 and in Princess Elizabeth Land (C-C') while elsewhere, the rates are very close to zero (except for the dynamically thinning glaciers). For 2010-2017 we see strong elevation gains in Dronning Maud Land and Enderby Land (A-B) but also strong losses in 2011. The mission lifetime of ICESat ended in 10/2009, CryoSat-2 provided the first measurements in 07/2010. Only Envisat covered both events but here, the orbit was shifted in 10/2010, resulting in different repeat track cells covered before and after the orbit shift. We merged all these missions as described in Sect. 3.3, which allows us to analyze the full time series. Comparing the elevation change from altimetry e.g. at point A in Fig.9c of 0.55±0.50 m with the change modeled using the FDM (0.48 m between 2008 and 2012) is a good example of successfully cross-validating these two data sets. Figure 8 shows the degree of agreement over the entire AIS.

As these elevation change rates alone do not contain any information on their origin, additional data are needed for improved process understanding. Figure 14 shows SEC rates for the interval 2002-2016 (March-September respectively) from altimetry and the FDM and respective rates of ice mass changes from GRACE. These maps show that the elevation gains in DML and Enderby Land agree very well with the firn model, which implies that increased snow accumulation during this period is responsible for the thickening. For Princess Elizabeth Land (C-C'). In the supplementary material Fig. S5 we calculated similar rates for the precipitation anomalies. These precipitation induced rates show a very consistent pattern compared to the elevation changes in East Antarctica. For the interval 2010-2017 they show that the strong mass losses in Princess Elizabeth Land can be related to a similar decline in precipitation. Also in Dronning Maud Land or Wilkes Land, the rates over the

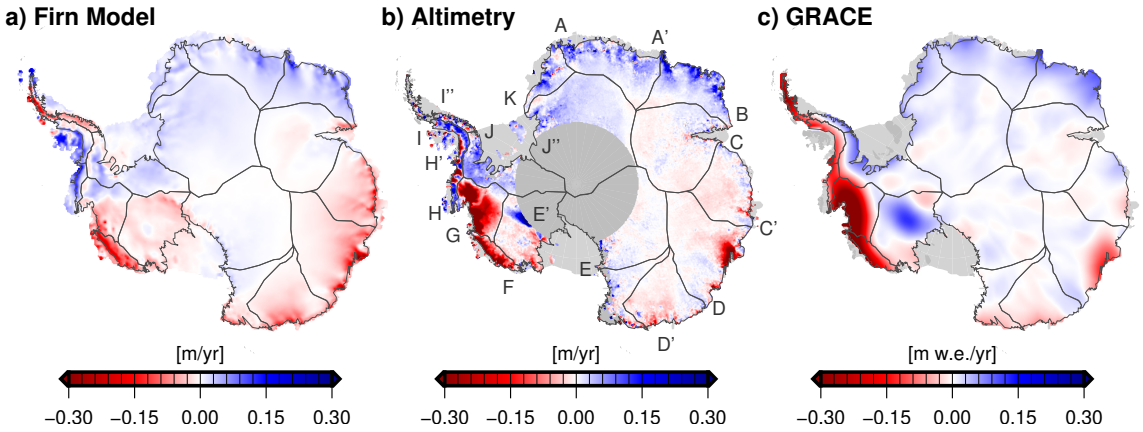

Figure 14. Mean rates for the time interval 2002-2016 of elevation changes from IMAU-FDM **(a)**, from the multi-mission SEC grids **(b)** and of the mass changes from GRACE **(c)**.

different intervals agree very well. In contrast, for West Antarctica, the patterns are significantly different which supports that the elevation changes are driven by ice dynamics here. Here, we can observe how the dynamic thinning has spread further inland during the last decade as described by Konrad et al. (2016). The strong variation between the different intervals points out that a linear rate over a decade may significantly differ from the long-term rate.

To cope with this interannual variation, we thus analyze the full time series of SEC, obtained after combining the single-mission time series as described in Sect. 3.3. Figure 6a shows five months as examples of the spatial coverage for the respective epochs. The profiles in Fig. 6b at different epochs show that in the southernmost part, which is located in the region of the subglacial Lake Vostok, the elevations vary by less than ±10, the negative rates agree as well, implying that the thinning here can be related to lower than normal snow accumulation. In contrast, the strong thinning along the Amundsen Sea Embayment (G-H) or the thickening of Kamb Ice Stream (E'-F) is not present in the FDM results but does show up in the GRACE data. Due to the higher densities of the involved material, ice dynamic processes show up even more pronounced in the map of mass changes, compared to the maps of elevation changes.

The inland propagation of dynamic thinning of the glaciers of the Amundsen Sea Embayment over the last decades has been described by Konrad et al. (2016). A recent onset of significant mass losses has also been reported for the adjacent glaciers along the Bellingshausen Sea (H-I, Wouters et al., 2015) and in the Getz and Abbot region (F-G, Chuter et al., 2017). Fig. over the last 25 years. Around kilometer 600 where the profile bends into the main flowline of Totten Glacier, we see a significantly rising elevation. The profiles at different epochs reveal that this is not a continuous change but that there is a distinct jump in the early 2000s. From the yearly precipitation anomaly maps (Fig.S8) we can see that in 2001 a strong snowfall event occurred in this region. At the very front of Totten Glacier, the elevation dropped by almost 12 from 1985 to 2010. Seasat could not successfully track a return signal near the front but the profile of 1978 shows that also before 1985, the glacier was already thinning. Between 2010 10i reveals that the largest losses along the coast of the WAIS occurred between 2007 and 2017, the

elevation decreased by more than 72012. The period 2012-2017 (Fig. . This means that the thinning accelerated from about 0.510i) shows that only a part of these large rates is persistent, indicating that also interannual variations in SMB have to be considered here (see also Chuter et al., 2017). The FDM-derived rate in Fig. to more than 1 in the last decade.These rates are consistent with the approximately 0.7 Flament and Rémy (2012) obtained from Envisat (2002-2010). Li et al. (2015) observe a grounding line retreat at Totten Glacier of 1 to 3 between 1996 and 2013 using SAR Interferometry. They conclude that this indicates an ice thinning of 12 (or 0.7) which is also very consistent with our results14a confirms the role of the surface mass balance in this region.

Summed up over larger regions the measurement noise is reduced and the time series reveal the losses and gains over the respective area. As can be seen from Fig.11a the sum of the Antarctic ice volume change is slightly negative over the last 25 years. This, however, is mainly a result of the accelerated dynamic thinning, especially in West Antarctica, over the last decade. Konrad et al. (2016) reported a spread as well as an amplification of the thinning of the glaciers along the Amundsen Sea Embayment (basin G-H). Since around 2007 to 2010, also the adjacent glaciers along the Bellingshausen Sea (H-H', Wouters et al., 2015) and in the Getz and Abbot region (F-G, Chuter et al., 2017) started to loose mass at steadily growing rates. The individual basin timeseries which can be found in the supplementary material confirm this increasing loss. Since the studyof Wouters et al. (2015), however, we observe that the region H'-I as well as the northernmost tip of the Peninsula (I-I") regained volume. Comparing the time series to anomalies in precipitation reveals that this can be explained by an extreme snowfall event

6.2 Ice sheet mass time series

The individual basin time series for these regions of the WAIS (in Fig. 12) allow us to analyze the increasing losses at a monthly resolution. They show that in 2004, the thinning of the Getz and Abbot region accelerated and experienced a further acceleration after 2007. After a small positive mass anomaly in late 2005, which relates to a similar event in the SMB time series, the overall mass losses in the Amundsen Sea Embayment accelerated. The Bellingshausen Sea basin was relatively stable until 2009, but started to lose significant amounts of mass after that time, as reported by Wouters et al. (2015). Since this study, however, we observe that the basins at the western part of the Peninsula (H-I) regained mass. The comparison with SMB reveals that this can be explained by a positive snowfall anomaly in this area in 2016. The shape and orientation of the Peninsula makes GRACE observations challenging with respect to leakage and GRACE error effects (Horwath and Dietrich, 2009). Nevertheless, the results of the satellite gravity mission confirm this anomaly as well. Here, the maps of differences in yearly averages help to discriminate the spatial pattern of the anomalies. In Fig.?? it becomes evident that an extreme snowfall event in 2016 occurred in western Palmer Land and northern Ellsworth Land, leading to this regain of volume. For the majority of the outlet glaciers in West Antarctica, the yearly differences in volume and precipitation do not agree very well. Instead, here, very persistent patterns of volume change can be observed , e.g. in the Amundsen Sea Embayment or at Kamb Ice Stream, which support the interpretation of a dynamic origin of these changes (Joughin et al., 1999; Pritchard et al., 2009). Furthermore, in Fig.11b and Fig. S6 b-f the mass time series from GRACE change at significantly larger rates compared to the volume time series. This also indicates that changes occur at remarkably higher densities. mass anomaly.

~~In contrast to West Antarctica,~~ The comparison of the ~~time series summed up over the East Antarctic Ice Sheet (EAIS) is even slightly positive (see Fig. 11b). As it can be seen from the individual basins (Fig. 13 and S7), the losses over the last decade at Totten Glacier (C'-D) and in George V Land (D-D') are compensated by volume gains in the remaining basins (A-C'). Here, the two early missions Seasat and Geosat help to extend the time series and thus get a better understanding of what is the long term behavior. Peaks and steps in the altimetry time series can be nicely related to corresponding events in the precipitation. We observe accumulation events in Dronning Maud Land (A-A') in 2002~~ice sheet wide mass time series between altimetry and GRACE in Fig. 11 reveals that for the WAIS, both datasets agree very well, ~~2009 and 2011. The yearly difference maps for SEC (Fig. **??**) and precipitation (Fig. S8) agree very well and show that, in 2002 the extreme snowfall occurred mainly in western Dronning Maud Land while in 2009 and 2011 the entire basin as well as the consecutive Enderby Land (A'-B) were affected. In Princess Elizabeth Land (C-C') and the catchment of Lambert Glacier, we observe the effect of a decreased precipitation in 1993 and 1994 which lead to a significant surface lowering. Conversely, in 2001/2002 a very strong snowfall event compensated these losses. Due to the large extend of these basins, this dent can even be detected in the time series over the entire Ice Sheet. Also in George V Land (D-D') the strong decrease in elevation between 2008 and 2010 is highly correlated to a deficit in accumulation. In this basin a difficulty in bridging the observational gap in the calibration of the old missions becomes evident. The altimetric elevations since 1992 show a linear behavior. Hence, we also use some data of this basin as described in Sect. 3.3 to determine the mean calibration bias of Seasat and Geosat. The precipitation anomalies confirm the linearity since the early nineties but they also show a significant change in the trend before. However, by using a mean calibration bias over entire Antarctica,~~ while for the APIS and the EAIS, significant differences are found. The percentage of observed area of the APIS (gray area in the background of Fig. 11d) indicates that before 2010 a significant part of the area remained unobserved. Here, conventional RA measurements very often failed due to the rugged terrain. Even for ICESat, the large across track distances and the ~~impact of this presumable non-linearity in the mission calibration is likely compensated by many different biases in other regions~~dependence on cloud-free conditions make measurements very sparse here. With the weather independent, dense and small footprint measurements of CryoSat-2 in SARIn mode, up to 80% of the area are covered by observations. Compared to GRACE, however, we observe a significantly weaker mass loss signal. Thomas et al. (2008) pointed out that RA fails to sample especially the large elevation changes in narrow valleys of outlet glaciers. This leads to an overall underestimation of the signal by altimetric observations. Even for ICESat this is true in this case, as cloudy conditions are not unusual in this region. But even when enough valid measurements would have been available, the fit of a planar surface over a diameter of 2 km would have been very challenging in the initial repeat altimetry processing here. Our approach is designed to provide valid observations over the majority of the AIS. Under the challenging conditions of the APIS, modifications such as a smaller diameter or more complex parametrization of the surface would surely help to improve the results. Furthermore, we did not calculate a SEC for cells that are further away than a beam-limited radar footprint from valid measurements. In order to interpolate or even extrapolate the results to unobserved cells, advanced gridding methods such as kriging, especially with the help of additional data sets (Hurkmans et al., 2012), would be advisable. In contrast, here we concentrate on the observed cells only.

The differences of the yearly averages of SEC in Fig.?? and the respective variations of precipitation in Fig. S8 reveal the spatial signature of the interannual variations. Even for the early missions Seasat and Geosat they show a very consistent picture and hence again demonstrate that these missions can provide important information to extend the observed time interval to a maximum.Between Seast and Geosat, we see elevations gains along the East Antarctic coast between 0°E and 70°E while west of the Amery Ice Shelf (70°E-150°E) the differences are negative. This is confirmed by the precipitation data for most of the area, even if the data here do not include 1978. Elevation gains in coastal western Enderby Land (40°E-50°E), which are very prominent in the precipitation data, are not well resolved by the early altimetry missions due to the distinct topography. Nevertheless, we see some positive elevation changes there too.In 1986, we observe a positive anomaly in Princess Elizabeth Land and Wilkes Landwhich coincides with an increased snowfall. A very similar spatial pattern repeats again in 1996, 2001, in 2004/2005 and in 2009. Mémin et al. (2015) already observed such periodic elevation anomalies using Envisat and calculated a frequency of 4.7 years. They identify the Antarctic Circumpolar Wave as a main driver for this periodic signal but also note that it is superimposed by ENSO. This might be the reason why in 2013 another occurrence, which would by expected by the periodicity, is unusually weak.

In contrast to the highly variable coastal regions, the interior of the EAIS is very stable. As it can be seen from Fig. 11e the surface in the LPZ varied between 5 and -8For the EAIS (Fig. during the last 25 years. A very slightly positive rate is consistent with the precipitation anomalies over this period. Zwally et al. (2015) observed a positive rate in this region as well and explain it by a continuing dynamic response to increased accumulation since the early Holocene. However, their estimated rate of about 211b) we see significant differences between the time series of mass changes from altimetry and from GRACE. For the time interval 2002 to 2016 (see Sect. would result in an elevation increase of 0.5F.3), the mean rate from altimetry (9.6±6.9 over the past 25 years, which clearly contradicts our results. Furthermore, kinematic GPS measurements on snowmobiles around Vostok station (Richter et al., 2014) yield an elevation change rate of 0.1Gt/yr) is mainly dominated by the accumulation events in 2009 and 2011. In contrast, the GRACE data imply an average mass gain of 42.1 0.5Gt/yr over this time interval. Especially after 2011, the differences become very prominent in the time series. The respective mass changes for the individual basins (Fig. for the period 2001 to 2013 which is in every good agreement with our altimetric time series12) reveal that this difference in the signals can be attributed to DML and Enderby Land. This might be a sign for dynamic thickening. Here, all elevation changes have been converted to mass using the density of surface firn. If a part of the positive elevation changes in this region indeed would be caused by ice dynamics, this would lead to an underestimation of mass gains from altimetry compared to gravimetric measurements. The results of the Bayesian combined approach of Martín-Español et al. (2017) also suggest a small dynamic thickening in this region. Rignot et al. (2008) observed no significant mass changes in this region between 1992 and 2006 using the input-output-method. Gardner et al. (2018) compared present day ice flow velocities to measurements from 2008. They obtain a slightly reduced ice discharge in DML (which would support the hypothesis of a dynamic thickening), while they observe a small increase in discharge for Enderby Land. Part of this misfit might also be explained by remaining processing issues in the GRACE processing (e.g. the GIA correction). Hence, we conclude that further work is needed to identify the origin of this discrepancy.

7 Conclusions

In this paper we presented an approach to combine different satellite altimetry missions, observation modes and techniques. The reprocessing of the conventional pulse limited radar altimetry ~~guarantees~~ ensures that two fundamental steps in processing of radar ice altimetry, the waveform retracking and the slope correction, are ~~handled consistently. Furthermore, we showed that the advanced methodsused in this processing improved the precision by up to~~ performed consistently. Furthermore, we showed that the advanced methods, used in this processing, improved the precision by more than 50%, compared to the widely used standard products. The validation with in situ measurements and the comparison with the IMAU-FDM shows that inter-mission offsets have been successfully corrected and that the uncertainty estimates for our resulting monthly multi-mission SEC grids are realistic.

~~From the combined time series of SEC~~ We analyzed the resulting time series and found that they provide detailed insight in the evolution of the surface elevation of the Antarctic Ice Sheet. From the combined SEC time series we calculated the long-term surface elevation change ~~rates~~ over the last 25 years. ~~In the coastal regions of East Antarctica we extended the time series back to~~ Due to Seasat and Geosat, observations in the coastal EAIS date back until 1978~~using the observations of the missions Seasat and Geosat. Hence, we were able to calculate the elevation change rates covering four decadesthere. Comparing rates calculated over different time intervals revealed which signals are persistent and where the interannual variations are dominant. The map of~~ , covering four decades. The unique data show that large parts of the East Antarctic plateau are very close to equilibrium, while changes over shorter time intervals identify interannual variations, which cannot be identified in long-term ~~trends, obtained from an unprecedented time interval, shows that large parts of the East Antarctic plateau are very close to equilibrium~~trends and are mostly associated with snowfall anomalies.

~~Besides the linear rates we were able to create monthly multi-mission time series which allow to study the evolution of the ice sheet volume over the full time span covered by any of the measurements. Peaks and steps in the altimetric SEC time series agree very well with the corresponding cumulated precipitation anomalies from ERA-Interim as well as the mass balance time series from GRACE. Note that we do not expect a perfect physical correlation between the three records. Making them fully comparable would require a sophisticated separation between surface and ice dynamic processes and the consideration of firn compaction (Ligtenberg et al., 2011; Li and Zwally, 2011). Both are beyond the scope of this paper. Nevertheless, the comparison of the different datasets shows, that our methodology successfully eliminated the biases between the different missions and observation techniques. We do not see any jumps in the time series, which could be interpreted as a calibration bias.~~

~~We conclude that this paper shows how to produce an altimetric elevation time series that is free of obvious artifacts of processing or calibration biases. This is essential to analyze the time series over the full time span of up to 40 years~~The monthly mass time series show that the AIS (excluding the polar gap within 81.5°S) lost an average amount of mass of -84.7±15.5 $\mathrm{Gt/yr}$ between 1992 and 2017. These losses accelerated in several regions and, hence, for 2010-2017 we obtain -137.0±24.9 $\mathrm{Gt/yr}$ for the same area. The comparison of the altimetry-derived mass changes, integrated over different basins and regions of the ice sheet, with SMB and GRACE shows high consistency of the different techniques. A correlation coefficient between the

mass anomalies from altimetry and from GRACE of 0.96 (for the time interval 2002-2016, see Tab. S4) indicates the excellent agreement of the observed interannual variations. The respective correlation with the SMB anomalies (0.60 for 1992-2016) is comparatively lower but still indicates a high agreement. In the APIS, differences between the mass time series of the different techniques arise mainly due to the poor spatial sampling of the altimetry data, while for the EAIS, the remaining discrepancies to mass time series from GRACE might be explained by the density mask used. These remaining issues and open questions should be addressed in future work in order to further reduce the uncertainty of the estimates of the mass balance of the AIS. The recently launched laser altimeter ICESat-2 promises a new milestone in ice sheet altimetry. We believe that our multi-mission combination approach can provide an important tool to combine the extremely high resolution of this mission with the long time period, covered by the previous missions.

Author contributions. L. Schröder designed the study and developed the PLRA reprocessing, the repeat altimetry processing and the time series generation. V. Helm supplied the reprocessed CryoSat-2 SARIn data. Stefan Ligtenberg and Michiel van den Broeke provided the RACMO and IMAU-FDM models. All authors discussed the results and contributed to the writing and editing of the manuscript.

Acknowledgements. This work is supported by the Deutsche Bundesstiftung Umwelt (DBU, German Federal Environmental Foundation). We thank the European Space Agency, the National Snow and Ice Data Center and the NASA Goddard Space Flight Center for providing the altimetry data products. Especially we would like to thank Jairo Santana for his support to access the GSFC data.

References

Armitage, T., Wingham, D., and Ridout, A.: Meteorological Origin of the Static Crossover Pattern Present in Low-Resolution-Mode CryoSat-2 Data Over Central Antarctica, IEEE Geosci. Remote Sens. Lett., 11, 1295–1299, https://doi.org/10.1109/LGRS.2013.2292821, 2014.

Arthern, R., Wingham, D., and Ridout, A.: Controls on ERS altimeter measurements over ice sheets: Footprint-scale topography, backscatter fluctuations, and the dependence of microwave penetration depth on satellite orientation, Journal of Geophysical Research – Atmospheres, 106, 33 471–33 484, 2001.

Bamber, J.: Ice Sheet Altimeter Processing Scheme, Int. J. Remote Sensing, 14, 925–938, 1994.

Bamber, J., Gomez-Dans, J., and Griggs, J.: A new 1 km digital elevation model of the Antarctic derived from combined satellite radar and laser data – Part 1: Data and methods, The Cryosphere, 3, 101–111, https://doi.org/10.5194/tc-3-101-2009, 2009.

Boening, C., Lebsock, M., Landerer, F., and Stephens, G.: Snowfall-driven mass change on the East Antarctic ice sheet, Geophys. Res. Lett., 39, L21 501, https://doi.org/10.1029/2012GL053316, 2012.

Brenner, A., Bindschadler, R., Zwally, H., and Thomas, R.: Slope-induced errors in radar altimetry over continental ice sheets, J. Geophys. Res., 88, 1617–1623, https://doi.org/10.1029/JC088iC03p01617, 1983.

Brenner, A., DiMarzio, J., and Zwally, H.: Precision and Accuracy of Satellite Radar and Laser Altimeter Data Over the Continental Ice Sheets, IEEE Trans. Geosci. Remote Sens., 45, 321–331, https://doi.org/10.1109/TGRS.2006.887172, 2007.

Brockley, D., Baker, S., Femenias, P., Martinez, B., Massmann, F.-H., Otten, M., Paul, F., Picard, B., Prandi, P., Roca, M., Rudenko, S., Scharroo, R., and Visser, P.: REAPER: Reprocessing 12 Years of ERS-1 and ERS-2 Altimeters and Microwave Radiometer Data, IEEE Trans. Geosci. Remote Sens., 55, 5506–5514, https://doi.org/10.1109/TGRS.2017.2709343, 2017.

Burton-Johnson, A., Black, M., Fretwell, P., and Kaluza-Gilbert, J.: An automated methodology for differentiating rock from snow, clouds and sea in Antarctica from Landsat 8 imagery: a new rock outcrop map and area estimation for the entire Antarctic continent, The Cryosphere, 10, 1665–1677, https://doi.org/10.5194/tc-10-1665-2016, 2016.

Chuter, S., Martín-Español, A., Wouters, B., and Bamber, J.: Mass balance reassessment of glaciers draining into the Abbot and Getz Ice Shelves of West Antarctica: Getz and Abbot Mass Balance Reassessment, Geophys. Res. Lett., 44, 7328–7337, https://doi.org/10.1002/2017GL073087, 2017.

Davis, C.: A Combined Surface/volume Scattering Retracking Algorithm for Ice Sheet Satellite Altimetry, in: Geoscience and Remote Sensing Symposium, 1992. IGARSS '92. International, vol. 2, pp. 969–971, https://doi.org/10.1109/IGARSS.1992.578311, 1992.

Davis, C.: A robust threshold retracking algorithm for measuring ice-sheet surface elevation change from satellite radar altimeters, Geoscience and Remote Sensing, IEEE Transactions on, 35, 974–979, https://doi.org/10.1109/36.602540, 1997.

Dee, D., Uppala, S., Simmons, A., Berrisford, P., Poli, P., Kobayashi, S., Andrae, U., Balmaseda, M., Balsamo, G., Bauer, P., Bechtold, P., Beljaars, A., van de Berg, L., Bidlot, J., Bormann, N., Delsol, C., Dragani, R., Fuentes, M., Geer, A., Haimberger, L., Healy, S., Hersbach, H., Hólm, E., Isaksen, L., Kållberg, P., Köhler, M., Matricardi, M., McNally, A., Monge-Sanz, B., Morcrette, J.-J., Park, B.-K., Peubey, C., de Rosnay, P., Tavolato, C., Thépaut, J.-N., and Vitart, F.: The ERA-Interim reanalysis: configuration and performance of the data assimilation system, Quart. J. R. Met. Soc., 137, 553–597, https://doi.org/10.1002/qj.828, 2011.

Flament, T. and Rémy, F.: Dynamic thinning of Antarctic glaciers from along-track repeat radar altimetry, J. Glac., 58, 830–840, 2012.

Frappart, F., Legrésy, B., Niño, F., Blarel, F., Fuller, N., Fleury, S., Birol, F., and Calmant, S.: An ERS-2 altimetry reprocessing compatible with ENVISAT for long-term land and ice sheets studies, Remote Sens. Environ., 184, 558–581, https://doi.org/10.1016/j.rse.2016.07.037, 2016.

Fricker, H. and Padman, L.: Thirty years of elevation change on Antarctic Peninsula ice shelves from multimission satellite radar altimetry, J. Geophys. Res., 117, https://doi.org/10.1029/2011JC007126, 2012.

Gardner, A., Moholdt, G., Scambos, T., Fahnstock, M., Ligtenberg, S., van den Broeke, M., and Nilsson, J.: Increased West Antarctic and unchanged East Antarctic ice discharge over the last 7 years, The Cryosphere, 12, 521–547, https://doi.org/10.5194/tc-12-521-2018, 2018.

Groh, A. and Horwath, M.: The method of tailored sensitivity kernels for GRACE mass change estimates, Geophys. Res. Abstr., 18, EGU2016–12 065, 2016.

Groh, A., Ewert, H., Scheinert, M., Fritsche, M., Rülke, A., Richter, A., Rosenau, R., and Dietrich, R.: An Investigation of Glacial Isostatic Adjustment over the Amundsen Sea sector, West Antarctica, Global Planet. Change, 98–99, 45–53, https://doi.org/10.1016/j.gloplacha.2012.08.001, 2012.

Gunter, B., Didova, O., Riva, R., Ligtenberg, S., Lenaerts, J., King, M., van den Broeke, M., and Urban, T.: Empirical estimation of present-day Antarctic glacial isostatic adjustment and ice mass change, The Cryosphere, 8, 743–760, https://doi.org/10.5194/tc-8-743-2014, 2014.

Helm, V., Humbert, A., and Miller, H.: Elevation and elevation change of Greenland and Antarctica derived from CryoSat-2, The Cryosphere, 8, 1539–1559, https://doi.org/10.5194/tc-8-1539-2014, 2014.

Hogg, A., Shepherd, A., Cornford, S., Briggs, K., Gourmelen, N., Graham, J., Joughin, I., Mouginot, J., Nagler, T., Payne, A., Rignot, E., and Wuite, J.: Increased ice flow in Western Palmer Land linked to ocean melting, Geophys. Res. Lett., 44, 4159–4167, https://doi.org/10.1002/2016GL072110, 2017.

Horwath, M. and Dietrich, R.: Signal and error in mass change inferences from GRACE: the case of Antarctica, Geophys. J. Int., 177, 849–864, https://doi.org/10.1111/j.1365-246X.2009.04139.x, 2009.

Horwath, M., Legrésy, B., Rémy, F., Blarel, F., and Lemoine, J.-M.: Consistent patterns of Antarctic ice sheet interannual variations from ENVISAT radar altimetry and GRACE satellite gravimetry, Geophys. J. Int., 189, 863–876, https://doi.org/10.1111/j.1365-246X.2012.05401.x, 2012.

Hurkmans, R., Bamber, J., Sørensen, L., Joughin, I., Davis, C., and Krabill, W.: Spatiotemporal interpolation of elevation changes derived from satellite altimetry for Jakobshavn Isbræ, Greenland, J. Geophys. Res., 117, https://doi.org/10.1029/2011JF002072, 2012.

Ivins, E., James, T., Wahr, J., O. Schrama, E., Landerer, F., and Simon, K.: Antarctic contribution to sea level rise observed by GRACE with improved GIA correction, J. Geophys. Res. Solid Earth, 118, 3126–3141, https://doi.org/10.1002/jgrb.50208, 2013.

Joughin, I., Gray, L., Bindschadler, R., Price, S., Morse, D., Hulbe, C., Mattar, K., and Werner, C.: Tributaries of West Antarctic Ice Streams Revealed by RADARSAT Interferometry, Science, 286, 283–286, 1999.

Joughin, I., Shean, D., Smith, B., and Dutrieux, P.: Grounding line variability and subglacial lake drainage on Pine Island Glacier, Antarctica, Geophys. Res. Lett., 43, 9093–9102, https://doi.org/10.1002/2016GL070259, 2016.

Kallenberg, B., Tregoning, P., Hoffmann, J., Hawkins, R., Purcell, A., and Allgeyer, S.: A new approach to estimate ice dynamic rates using satellite observations in East Antarctica, The Cryosphere, 11, 1235–1245, https://doi.org/10.5194/tc-11-1235-2017, 2017.

Khvorostovsky, K.: Merging and Analysis of Elevation Time Series Over Greenland Ice Sheet From Satellite Radar Altimetry, IEEE Trans. Geosci. Remote Sens., 50, 23–36, https://doi.org/10.1109/TGRS.2011.2160071, 2012.

Konrad, H., Gilbert, L., Cornford, S., Payne, A., Hogg, A., Muir, A., and Shepherd, A.: Uneven onset and pace of ice-dynamical imbalance in the Amundsen Sea Embayment, West Antarctica, Geophys. Res. Lett., https://doi.org/10.1002/2016GL070733, 2016.

Lacroix, P., Dechambre, M., Legrésy, B., Blarel, F., and Rémy, F.: On the use of the dual-frequency ENVISAT altimeter to determine snowpack properties of the Antarctic ice sheet, Remote Sens. Environ., 112, 1712–1729, https://doi.org/10.1016/j.rse.2007.08.022, 2008.

Legrésy, B. and Rémy, F.: Altimetric observations of surface characteristics of the Antarctic ice sheet, J. Glac., 43, 265–276, 1997.

Legrésy, B., Rémy, F., and Schaeffer, P.: Different ERS altimeter measurements between ascending and descending tracks caused by wind induced features over ice sheets, Geophys. Res. Lett., 26, 2231–2234, https://doi.org/10.1029/1999GL900531, 1999.

Legrésy, B., Papa, F., Rémy, F., Vinay, G., van den Bosch, M., and Zanife, O.-Z.: ENVISAT radar altimeter measurements over continental surfaces and ice caps using the ICE-2 retracking algorithm, Remote Sens. Environ., 85, 150–163, https://doi.org/10.1016/j.rse.2004.11.018, 2005.

Legrésy, B., Rémy, F., and Blarel, F.: Along track repeat altimetry for ice sheets and continental surface studies, in: Proc. Symposium on 15 years of Progress in Radar Altimetry, Venice, Italy, 13–18 March 2006, European Space Agency Publication Division, Noordwijk, The Netherlands, eSA-SP No. 614, paper No. 181, 2006.

Lenaerts, J., van Meijgaard, E., van den Broeke, M., Ligtenberg, S., Horwath, M., and Isaksson, E.: Recent snowfall anomalies in Dronning Maud Land, East Antarctica, in a historical and future climate perspective, Geophys. Res. Lett., 40, 2684–2688, https://doi.org/10.1002/grl.50559, 2013.

Li, J. and Zwally, H.: Modeling of firn compaction for estimating ice-sheet mass change from observed ice-sheet elevation change, Ann. Glac., 52, 1–7, https://doi.org/10.3189/172756411799096321, 2011.

Li, X., Rignot, E., Morlighem, M., Mouginot, J., and Scheuchl, B.: Grounding line retreat of Totten Glacier, East Antarctica, 1996 to 2013, Geophys. Res. Lett., 42, 8049–8056, https://doi.org/10.1002/2015GL065701, 2015.

Li, X., Rignot, E., Mouginot, J., and Scheuchl, B.: Ice flow dynamics and mass loss of Totten Glacier, East Antarctica, from 1989 to 2015, Geophys. Res. Lett., 43, 6366–6373, https://doi.org/10.1002/2016GL069173, 2016.

Li, Y. and Davis, C.: Decadal Mass Balance of the Greenland and Antarctic Ice Sheets from High Resolution Elevation Change Analysis of ERS-2 and Envisat Radar Altimetry Measurements, in: IEEE International Geoscience & Remote Sensing Symposium, IGARSS 2008, July 8-11, 2008, Boston, Massachusetts, USA, Proceedings, pp. 339–342, IEEE, https://doi.org/10.1109/IGARSS.2008.4779727, 2008.

Ligtenberg, S., Helsen, M., and van den Broeke, M.: An improved semi-empirical model for the densification of Antarctic firn, The Cryosphere, 5, 809–819, https://doi.org/10.5194/tc-5-809-2011, 2011.

Martin, T., Zwally, H., Brenner, A., and Bindschadler, R.: Analysis and retracking of continental ice sheet radar altimeter waveforms, J. Geophys. Res., 88, 1608, https://doi.org/10.1029/JC088iC03p01608, 1983.

Martín-Español, A., Bamber, J., and Zammit-Mangion, A.: Constraining the mass balance of East Antarctica, Geophys. Res. Lett., 44, https://doi.org/10.1002/2017GL072937, 2017.

McMillan, M., Shepherd, A., Sundal, A., Briggs, K., Muir, A., Ridout, A., Hogg, A., and Wingham, D.: Increased ice losses from Antarctica detected by CryoSat-2, Geophys. Res. Lett., 41, 3899–3905, https://doi.org/10.1002/2014GL060111, 2014.

McMillan, M., Leeson, A., Shepherd, A., Briggs, K., Armitage, T., Hogg, A., Kuipers Munneke, P., van den Broeke, M., Noël, B., van de Berg, W., Ligtenberg, S., Horwath, M., Groh, A., Muir, A., and Gilbert, L.: A high-resolution record of Greenland mass balance, Geophys. Res. Lett., 43, 7002–7010, https://doi.org/10.1002/2016GL069666, 2016.

Mémin, A., Flament, T., Alizier, B., Watson, C., and Rémy, F.: Interannual variation of the Antarctic Ice Sheet from a combined analysis of satellite gravimetry and altimetry data, Earth Planet. Sci. Lett., 422, 150–156, https://doi.org/10.1016/j.epsl.2015.03.045, 2015.

Mouginot, J., Rignot, E., and Scheuchl, B.: Sustained increase in ice discharge from the Amundsen Sea Embayment, West Antarctica, from 1973 to 2013, Geophys. Res. Lett., 41, 1576–1584, https://doi.org/10.1002/2013GL059069, 2014.

Nilsson, J., Vallelonga, P., Simonsen, S., Sørensen, L., Forsberg, R., Dahl-Jensen, D., Hirabayashi, M., Goto-Azuma, K., Hvidberg, C., Kjaer, H., and Satow, K.: Greenland 2012 melt event effects on CryoSat-2 radar altimetry, Geophys. Res. Lett., 42, 3919–3926, https://doi.org/10.1002/2015GL063296, 2015.

Nilsson, J., Gardner, A., Sandberg Sørensen, L., and Forsberg, R.: Improved retrieval of land ice topography from CryoSat-2 data and its impact for volume-change estimation of the Greenland Ice Sheet, The Cryosphere, 10, 2953–2969, https://doi.org/10.5194/tc-10-2953-2016, 2016.

Paolo, F., Fricker, H., and Padman, L.: Constructing improved decadal records of Antarctic ice shelf height change from multiple satellite radar altimeters, Remote Sens. Environ., 177, 192–205, https://doi.org/10.1016/j.rse.2016.01.026, 2016.

Pritchard, H., Arthern, R., Vaughan, D., and Edwards, L.: Extensive dynamic thinning on the margins of the Greenland and Antarctic ice sheets, Nature, 461, 971–975, https://doi.org/10.1038/nature08471, 2009.

Rémy, F. and Parouty, S.: Antarctic Ice Sheet and Radar Altimetry: A Review, Remote Sensing, 1, 1212–1239, https://doi.org/10.3390/rs1041212, 2009.

Richter, A., Popov, S., Dietrich, R., Lukin, V., Fritsche, M., Lipenkov, V., Matveev, A., Wendt, J., Yuskevich, A., and Masolov, V.: Observational evidence on the stability of the hydro-glaciological regime of subglacial Lake Vostok, Geophys. Res. Lett., 35, L11 502, https://doi.org/10.1029/2008GL033397, 2008.

Richter, A., Popov, S., Fritsche, M., Lukin, V., Matveev, A., Ekaykin, A., Lipenkov, V., Fedorov, D., Eberlein, L., Schröder, L., Ewert, H., Horwath, M., and Dietrich, R.: Height changes over subglacial Lake Vostok, East Antarctica: Insights from GNSS observations, J. Geophys. Res. Earth Surf., 119, 2460–2480, https://doi.org/10.1002/2014JF003228, 2014.

Rignot, E.: Changes in ice dynamics and mass balance of the Antarctic ice sheet, Phil. Trans. R. Soc. Lond. A, 364, 1637–1655, 2006.

Rignot, E., Bamber, J., van den Broeke, M., Davis, C., Li, Y., van de Berg, W., and van Meijgaard, E.: Recent Antarctic ice mass loss from radar interferometry and regional climate modelling, Nature Geosci., 1, 106–110, https://doi.org/10.1038/ngeo102, 2008.

Rignot, E., Mouginot, J., and Scheuchl, B.: Ice Flow of the Antarctic Ice Sheet, Science, 333, 1427–1430, https://doi.org/10.1126/science.1208336, 2011.

Rignot, E., Mouginot, J., Morlighem, M., Seroussi, H., and Scheuchl, B.: Widespread, rapid grounding line retreat of Pine Island, Thwaites, Smith, and Kohler glaciers, West Antarctica, from 1992 to 2011, Geophys. Res. Lett., 41, 3502–3509, https://doi.org/10.1002/2014GL060140, 2014.

Roemer, S., Legrésy, B., Horwath, M., and Dietrich, R.: Refined analysis of radar altimetry data applied to the region of the subglacial Lake Vostok / Antarctica, Remote Sens. Environ., 106, 269–284, https://doi.org/10.1016/j.rse.2006.02.026, 2007.

Schröder, L., Richter, A., Fedorov, D., Eberlein, L., Brovkov, E., Popov, S., Knöfel, C., Horwath, M., Dietrich, R., Matveev, A., Scheinert, M., and Lukin, V.: Validation of satellite altimetry by kinematic GNSS in central East Antarctica, The Cryosphere, 11, 1111–1130, https://doi.org/10.5194/tc-11-1111-2017, 2017.

Scott, R., Baker, S., Birkett, C., Cudlip, W., Laxon, S., Mantripp, D., Mansley, J., Morley, J., Rapley, C., Ridley, J., Strawbridge, F., and Wingham, D.: A comparison of the performance of the ice and ocean tracking modes of the ERS-1 radar altimeter over non-ocean surfaces, Geophys. Res. Lett., 21, 553–556, https://doi.org/10.1029/94GL00178, 1994.

Shepherd, A., Ivins, E., A, G., Barletta, V., Bentley, M., Bettadpur, S., Briggs, K., Bromwich, D., Forsberg, R., Galin, N., Horwath, M., Jacobs, S., Joughin, I., King, M., Lenaerts, J., Li, J., Ligtenberg, S., Luckman, A., Luthcke, S., McMillan, M., Meister, R., Milne, G., Mouginot, J., Muir, A., Nicolas, J., Paden, J., Payne, A., Pritchard, H., Rignot, E., Rott, H., Sorensen, L., Scambos, T., Scheuchl, B., Schrama, E., Smith, B., Sundal, A., van Angelen, J., van de Berg, W., van den Broeke, M., Vaughan, D., Velicogna, I., Wahr, J., Whitehouse, P., Wingham, D., Yi, D., Young, D., and Zwally, H.: A Reconciled Estimate of Ice-Sheet Mass Balance, Science, 338, 1183–1189, https://doi.org/10.1126/science.1228102, 2012.

Shepherd, A., Ivins, E., Rignot, E., Smith, B., van den Broeke, M., Velicogna, I., Whitehouse, P., Briggs, K., Joughin, I., Krinner, G., Nowicki, S., Payne, T., Scambos, T., Schlegel, N., A, G., Agosta, C., Ahlstrøm, A., Babonis, G., Barletta, V., Blazquez, A., Bonin, J., Csatho, B., Cullather, R., Felikson, D., Fettweis, X., Forsberg, R., Gallee, H., Gardner, A., Gilbert, L., Groh, A., Gunter, B., Hanna, E., Harig, C., Helm, V., Horvath, A., Horwath, M., Khan, S., Kjeldsen, K., Konrad, H., Langen, P., Lecavalier, B., Loomis, B., Luthcke, S., McMillan, M., Melini, D., Mernild, S., Mohajerani, Y., Moore, P., Mouginot, J., Moyano, G., Muir, A., Nagler, T., Nield, G., Nilsson, J., Noel, B., Otosaka, I., Pattle, M., Peltier, W., Pie, N., Rietbroek, R., Rott, H., Sandberg-Sørensen, L., Sasgen, I., Save, H., Scheuchl, B., Schrama, E., Schröder, L., Seo, K.-W., Simonsen, S., Slater, T., Spada, G., Sutterley, T., Talpe, M., Tarasov, L., van de Berg, W., van der Wal, W., van Wessem, M., Vishwakarma, B., Wiese, D., and Wouters, B.: Mass balance of the Antarctic Ice Sheet from 1992 to 2017, Nature, 558, 219–222, https://doi.org/10.1038/s41586-018-0179-y, 2018.

Simonsen, S. and Sørensen, L.: Implications of changing scattering properties on Greenland ice sheet volume change from Cryosat-2 altimetry, Remote Sens. Environ., 190, 207–216, https://doi.org/10.1016/j.rse.2016.12.012, 2017.

Sørensen, L., Simonsen, S., Nielsen, K., Lucas-Picher, P., Spada, G., Adalgeirsdottir, G., Forsberg, R., and Hvidberg, C.: Mass balance of the Greenland ice sheet (2003–2008) from ICESat data – the impact of interpolation, sampling and firn density, The Cryosphere, 5, 173–186, https://doi.org/10.5194/tc-5-173-2011, 2011.

Studinger, M.: IceBridge ATM L4 Surface Elevation Rate of Change, Version 1. Updated 2017., Boulder, Colorado USA. NASA National Snow and Ice Data Center Distributed Active Archive Center, https://doi.org/10.5067/BCW6CI3TXOCY, [date accessed: 2018-02-28], 2014.

Thomas, E., Hosking, J., Tuckwell, R., Warren, R., and Ludlow, E.: Twentieth century increase in snowfall in coastal West Antarctica, Geophys. Res. Lett., 42, 9387–9393, https://doi.org/10.1002/2015GL065750, 2015.

Thomas, R., Davis, C., Frederick, E., Krabill, W., Li, Y., Manizade, S., and Martin, C.: A comparison of Greenland ice-sheet volume changes derived from altimetry measurements, J. Glac., 54, 203–212, https://doi.org/10.3189/002214308784886225, 2008.

van Wessem, J., van de Berg, W., Noël, B., van Meijgaard, E., Amory, C., Birnbaum, G., Jakobs, C., Krüger, K., Lenaerts, J., Lhermitte, S., Ligtenberg, S., Medley, B., Reijmer, C., van Tricht, K., Trusel, L., van Ulft, L., Wouters, B., Wuite, J., and van den Broeke, M.: Modelling the climate and surface mass balance of polar ice sheets using RACMO2 – Part 2: Antarctica (1979–2016), The Cryosphere, 12, 1479–1498, https://doi.org/10.5194/tc-12-1479-2018, 2018.

Wingham, D., Rapley, C., and Griffiths, H.: New techniques in satellite altimeter tracking systems, in: ESA Proceedings of the 1986 International Geoscience and Remote Sensing Symposium(IGARSS'86) on Remote Sensing: Today's Solutions for Tomorrow's Information Needs,, vol. 3, pp. 1339–1344, 1986.

Wingham, D., Ridout, A., Scharroo, R., Arthern, R., and Shum, C.: Antarctic Elevation Change from 1992 to 1996, Science, 282, 456–458, https://doi.org/10.1126/science.282.5388.456, 1998.

Wingham, D., Francis, C., Baker, S., Bouzinac, C., Brockley, D., Cullen, R., Chateau-Thierry, P. d., Laxon, S., Mallow, U., Mavrocordatos, C., Phalippou, L., Ratier, G., Rey, L., Rostan, F., Viau, P., and Wallis, D.: CryoSat: A mission to determine the fluctuations in Earth's land and marine ice fields, Adv. Space Res., 37, 841–871, https://doi.org/10.1016/j.asr.2005.07.027, 2006a.

Wingham, D., Shepherd, A., Muir, A., and Marshall, G.: Mass balance of the Antarctic ice sheet, Phil. Trans. R. Soc. Lond. A, 364, 1627–1635, https://doi.org/10.1098/rsta.2006.1792, 2006b.

Wouters, B., Bamber, J., van den Broeke, M., Lenaerts, J., and Sasgen, I.: Limits in detecting acceleration of ice sheet mass loss due to climate variability, Nature Geosci., 6, 613–616, https://doi.org/10.1038/ngeo1874, 2013.

Wouters, B., Martín-Español, A., Helm, V., Flament, T., van Wessem, J., Ligtenberg, S., van den Broeke, M., and Bamber, J.: Dynamic thinning of glaciers on the Southern Antarctic Peninsula, Science, 348, 899–903, https://doi.org/10.1126/science.aaa5727, 2015.

Zwally, H., Giovinetto, M., Li, J., Cornejo, H., Beckley, M., Brenner, A., Saba, J., and Yi, D.: Mass changes of the Greenland and Antarctic ice sheets and shelves and contributions to sea-level rise: 1992-2002, J. Glac., 51, 509–527, https://doi.org/10.3189/172756505781829007, 2005.

Zwally, H., Li, J., Robbins, J., Saba, J., Yi, D., and Brenner, A.: Mass gains of the Antarctic ice sheet exceed losses, J. Glac., 61, 1019–1936, 2015.